CHALMERS
UNIVERSITY OF TECHNOLOGY

Motion prediction and control of a tractor-semitrailer combination to detect and prevent jackknifing

Master's thesis in Systems, Control and Mechatronics

SHENGTING XIE
SIXUAN PEI

DEPARTMENT OF ELECTRICAL ENGINEERING

CHALMERS UNIVERSITY OF TECHNOLOGY
Gothenburg, Sweden 2024
www.chalmers.se

Master's thesis 2024

Motion prediction and control of a tractor-semitrailer combination to detect and prevent jackknifing

SHENGTING XIE
SIXUAN PEI

CHALMERS
UNIVERSITY OF TECHNOLOGY

Department of Electrical Engineering
Division of Systems and Control
Chalmers University of Technology
Gothenburg, Sweden 2024

Motion prediction and control of a tractor-semitrailer combination to detect and prevent jackknifing
SHENGTING XIE
SIXUAN PEI

Supervisor:
Maliheh Sadeghi Kati, Volvo Group Trucks Technology
Umur Erdinc, Volvo Group Trucks Technology
Leo Laine, Volvo Group Trucks Technology
Mats Jonasson, Chalmers Department of Mechanics and Maritime Sciences
Jonas Fredriksson, Chalmers Department of Electrical Engineering

Examiner:
Jonas Fredriksson, Chalmers Department of Electrical Engineering

Master's Thesis 2024
Department of Electrical Engineering
Division of Systems and Control
Chalmers University of Technology
SE-412 96 Gothenburg
Telephone +46 31 772 1000

Cover: Visualization of Cornering Dynamics of a Tractor Semi-Trailer.

Typeset in LaTeX
Gothenburg, Sweden 2024

Motion prediction and control of a tractor-semitrailer combination to detect and prevent jackknifing
SHENGTING XIE
SIXUAN PEI
Department of Electrical Engineering
Chalmers University of Technology

Abstract

This thesis explores the motion prediction of articulated heavy vehicles (AHV), specifically focusing on jackknifing instability, a leading cause of severe traffic accidents. The thesis focuses on developing a comprehensive prediction algorithm to anticipate and mitigate jackknifing events. The study critically assesses the applicability of two different mathematical descriptions of the vehicle's dynamics in capturing jackknifing. These models' correctness and limitations are identified by comparing the simulation results with the Volvo Transport Model (VTM). The motion prediction algorithm is devised to predict the motion of the AHV. It employs a discrete state space model and driver input prediction methods, enabling timely prediction for potential jackknifing scenarios. The algorithm's effectiveness is validated through high-fidelity simulations using VTM. Furthermore, the study introduces a jackknifing indicator and trailer braking strategy, together with the motion prediction algorithms, to design a safety system capable of preventing jackknifing. In conclusion, by incorporating the prediction algorithms, a jackknifing indicator, and a trailer braking strategy, a safety system that can predict, prevent, and mitigate the risks associated with jackknifing has been successfully developed.

Acknowledgements

We want to express our sincere thanks to Jonas Fredriksson, our examiner, for continuously providing us with valuable feedback and input for our thesis. We are truly grateful to our supervisors Maliheh Sadeghi Kati, Umur Erdinc, Esteban Gelso, Mats Jonasson, Leo Laine for their invaluable insights, guidance, and constructive comments that have significantly enriched our work. We also want to acknowledge the support and active participation of our colleagues Cecilia Bustrén, Salmane Essayeh, who patiently answered our questions and doubts that have been instrumental in our progress. Additionally, we would like to extend thanks to our colleague Basar Özkan whose willingness to assist has consistently made our journey more enjoyable.

List of Acronyms

Below is the list of acronyms that have been used throughout this thesis listed in alphabetical order:

AHV	Articulated Heavy Vehicles
ABS	Anti-lock Braking Systems
CoG	Center of Gravity
ESC	Electronic Stability Control
GTT	Volvo Group Trucks Technology
MBS	Multi-body System
RSC	Roll Stability Control
VTM	Volvo Transport Model
VMM	Vehicle Motion Management

Nomenclature

Below is the nomenclature of indices, parameters, and variables that have been used throughout this thesis.

Indices

i	Index for vehicle unit
j	Index for unit axle
k	Index can take on the values "l" for left or "r" for right. For single-track model "k" does not exist
req	Request
act	Actuator
$ctrl$	Slip controller
$pred$	Predicted
ref	Reference

Parameters

xa	The displacement vector from the CoG position to the axle
xc	The positions of the coupling points relative to the center of gravity (COG) of the unit
m	Mass of unit
g	Gravitational acceleration
μ	Friction coefficient
c_y	Normalized equivalent cornering stiffness
I_z	Unit's yaw moment of inertia
r	Rolling radius of the tire
F_{xair}	Air resistance force acting on the tractor's front cross-section.

A_f	Frontal area of the tractor
C_d	Drag coefficient
ρ_{air}	Air density
e	The scaling factor that defines conservativity of the friction circle-inspired combined slip model
tw	Track width
J	Yaw moment of inertia of unit
Δh	Redundant geometric parameter
hr	Height of the axle roll center
cr	Axle's roll stiffness
L_{2r}	Grouped axle distance to the CoG of the trailer
L_{2f}	Grouped axle distance to the coupling point
L_i	Wheel base length of i^{th} unit
K_p	Proportional gain for the speed controller
K_i	Integral gain for the speed controller
τ	Time constant
br	Ratio of brake force on each axle when applying the trailer braking
T_s	The sampling period
$Horzion$	The total number of future time steps for prediction
nc	The number of generalized coordinates
nf	The number of force elements

Variables

v_x	Longitudinal speed of unit in the local frame of the truck
v_y	Lateral velocity of the CoG of the unit in the local frame of the truck.
ϕ	Heading angle (yaw angle) of the unit in the global frame
$\dot{\phi}$	Yaw rate of the unit
θ	Articulation angle between the tractor and the semi-trailer
$\dot{\theta}$	Rate of articulation angle between the tractor and the semi-trailer
F_{xw}	Longitudinal force
δ	Steering angle of the tractor's front axle
$T_{kinetic}$	Total kinetic energy of the system.

V	Total potential energy of the system.
Q	Generalized forces acting on the system.
q	Generalized coordinates describing position and orientation.
nl	Index for the chosen generalized coordinates.
X	Position on the yaw plane in the global coordinates in the x direction.
Y	Position on the yaw plane in the global coordinates in the y direction.
s_y	Lateral slip
s_x	Longitudinal slip
F_{yw}	Lateral forces on the wheels
F_{xw}	Longitudinal forces on the wheels
F_Z	Vertical load on the wheels considering lateral load transfer
p	Position vector of the point where the force element acts on
u	Driver input vector to the model
x	State vector of the vehicle
F_{vcx}	Vehicle coupling force in the vehicle frame along the x direction
F_{vcy}	Vehicle coupling force in the vehicle frame along the y direction
F_{gcx}	Vehicle coupling force in the global frame along the x direction
F_{gcy}	Vehicle coupling force in the global frame along the y direction
F_z	Vertical load without considering lateral load transfer
F_Z	Vertical load considering both longitudinal load transfer and vertical load transfer
F_{cz}	Vertical load on the vehicle coupling point without considering lateral load transfer
a_x	Acceleration of the unit along the x direction
a_y	Acceleration of the unit along the y direction
F_{lat}	The amount of lateral load transfer
T	Torque
s	The complex frequency variable in the Laplace domain
$G(s)$	The transfer function
n	The discrete-time index
M	The future time step
Φ	The factor responsible for reducing the maximum lateral forces that the tire model can generate

Contents

List of Figures

List of Tables

1
Introduction

1.1 Background

Articulated heavy vehicles (AHVs) are widely used in transportation systems due to their capacity to carry heavy goods. The weights and sizes of AHVs are significant, which benefits the carrying capacity, but at the same time, these features can cause catastrophic accidents when AHVs are involved in accidents. This causes threats to the safety of both the truck driver and other road users. In the United States, around 35000 people died in road accidents, and about 10% of them died due to unstable motion of AHVs [1].

Vehicle instability can lead to the loss of control of AHVs. Typical instability modes are trailer swing (trailer snaking), jackknifing, and roll-over, which all present significant threats to driving safety. Jackknifing arises primarily due to saturated friction force between the tractor's rear tires and the ground [2]. It typically occurs during abrupt braking or when the vehicle traverses a curved path. It is noteworthy that jackknifing is most frequently observed when the semi-trailer is empty [3].

Trailer swing is another mode of unstable motion, characterized by the lateral movement of the trailer moving from one side to the other side behind the towing tractor. In the event of trailer skidding, the trailer can exert a pushing force on the towing vehicle and spin the towing vehicle around, eventually leading to loss of control.

Jackknifing is a severe yaw instability situation characterized by a significant heading angle error between the towing unit and the intended path direction. This phenomenon occurs when the towing unit loses lateral tire grip, leading to sideways sliding. On wet and slippery roads, during braking conditions, the occurrence of wheel blockage can lead to jackknifing of the vehicle [4]. The insufficiency of lateral forces generated by the brake tire predominantly causes the jackknifing problem.

The free-rolling wheel can provide lateral force due to the wheel's side slip angle and cornering stiffness. An increase in longitudinal slip generates a brake force and concurrently reduces the lateral force. Consequently, a shift in longitudinal slip induces a directional alteration in the resulting wheel forces, leading to a modification in the yaw moment [5]. It is undeniable that lateral forces from wheels play a pivotal role in maintaining the vehicle's stability while cornering. If the total lateral forces on the tractor are insufficient, jackknifing will likely occur. Similarly, inadequate

lateral forces on the trailer's tires lead to trailer swing.

The role of vertical load transfer on the wheels warrants consideration within this context. One key factor influencing the lateral forces generated by each tire is the combined slip effect. Primarily, vehicle yaw instability arises due to tire saturation [6]. Combined slip arises due to the interaction between longitudinal and lateral tire forces when a vehicle simultaneously brakes or accelerates while cornering. The resulting force from the interaction of these two forces must not surpass the friction limit, which equals the product of the wheel's vertical load and the friction coefficient.

To address yaw instability problems, active safety systems such as Roll Stability Control (RSC), Electronic Stability Control (ESC), and Anti-lock Braking Systems (ABS) have been developed and investigated to improve vehicle directional stability. These systems primarily operate by continuously monitoring different stability indicators and intervening to maintain the directional stability of the vehicle [7]. Such safety systems are classified as "reactive safety systems" and primarily focus on reacting to the current vehicle situation [8]. However, relying solely on these systems might not ensure safety, as the response could be too late, potentially leading to a complete loss of directional stability before the system engages. Furthermore, these systems use the conventional braking system on all wheels to maintain stability.

During braking of an electric vehicle, the electric axle can convert the mechanical energy to electricity, while braking the non-powered axle converts mechanical energy to heat. Solely braking the powered axle can maximize the regenerative energy. However, it increases the risk of jackknifing. One approach to mitigate the risk of jackknifing involves anticipating future driver behavior. By doing so, it might be possible to take proactive measures to prevent vehicle instability from occurring initially while converting sufficient mechanical energy to electricity.

1.2 Purpose

This thesis aims to develop a safety system that can predict and mitigate the potential occurrence of jackknifing in articulated vehicles. The safety system should monitor the state of the articulated vehicle while maintaining a continuous prediction of driver behavior. Guided by a specific jackknifing indicator, the safety system should predict jackknifing proactively and prevent the vehicle from entering a jackknife state.

1.3 Objective

The following objects are set up to fulfill the purpose of the thesis.

- Construct a suitable force-based model for an articulated vehicle that yields simulation results closely aligned with VTM (Volvo Transport Models), par-

ticularly in cases that involve truck jackknifing incidents.

- Incorporate a prediction method for driver behavior to forecast future inputs, including steering angles and brake forces.

- Utilize the driver behavior prediction and force-based model to create a prediction model for anticipating the dynamics of an articulated vehicle motion in the near future.

- Identify and define a proper method for detecting jackknifing, along with establishing thresholds capable of indicating the occurrence of such events.

- Implement preventive measures to avoid jackknifing based on predictions made by the prediction model.

1.4 Scope

The scope of the thesis is limited to a specific AHV configuration. The studied vehicle includes a 4×2 tractor and a 4×0 trailer, forming a tractor semi-trailer combination. The tractor's front axle is steerable and longitudinal tire forces on all wheels are assumed to be controllable. The parameters of this AHV align with those of a tractor-trailer model in the Volvo Transport Model (VTM) library. The dynamic model holds validity only on horizontal ground and the road friction coefficient of 0.3 is assumed. The dynamic model ignores the impact of strong wind gusts that can influence the vehicle's motion and rolling resistance. Parameters such as the air density ρ_{air}, the projected area in the direction of motion A_f, and the drag coefficient C_d are constants. The model includes a slip controller that maintains the longitudinal slip of the wheels within a narrow threshold of 0.1. The slip controller can supply the requested longitudinal force for each wheel and enhance the safety system's jackknifing prediction by equipping a more cautious dynamic model.

1.5 Disposition

This thesis investigates the design and implementation of a jackknifing prevention system for a specific tractor-semi-trailer combination. The objective is to improve the yaw stability of AHVs by predicting and preventing jackknifing occurrences. The following paragraph highlights the key components of each chapter in the research.

Chapter 1 introduces the background and context of AHVs, highlighting the need for an improved safety system capable of preventing jackknife. The purpose and objectives of the research are defined, focusing on developing a jackknifing prevention system. The scope of the study and the thesis disposition are presented. Chapter 2 explores motion models used for the articulated vehicle dynamics analysis. Two vehicle dynamic models, a single-track model and a two-track model with load transfer, are introduced. The tire model that simulates the VTM is also explained. The

high-fidelity model VTM is described and the validation of single and two-track models with VTM is done. Chapter 3 details the design and implementation of the proposed safety system. The discretization processes for both single-track and two-track models are then presented. After that, chapter 3 explores the predictor module, outlines its role in forecasting driver behavior, including steering and tire forces input, and presents the methodology for predicting jackknifing occurrences and measures to prevent them. Chapter 4 presents the results of the simulation experiments conducted to validate and evaluate the safety system. The test cases and the predictions from single-track and two-track models are discussed. Insights into the safety system's effectiveness in enhancing vehicle directional stability are provided. Chapter 5 summarizes the research findings and identifies potential areas for future research.

2
Modeling

The prediction algorithms utilize a force-based model to predict the motion of the tractor-semi-trailer combination. The model needs to be computationally efficient to enable real-time prediction. Moreover, the model must exhibit sufficient accuracy to capture jackknife events when a severe driver maneuver has been taken, such as excessive steering angle or strong braking in a curve on a low-friction road surface.

This chapter starts with steps for modeling the 4×2 tractor and 4×0 semi-trailer combination. Two different approaches are applied to modeling the motion of the tractor-trailer: a kinetic single-track model formalized by a Lagrangian method and a kinetic two-track model formalized by a Newtonian method.

After the modeling sections, both models are validated using several driver maneuver input signals against a more complex model, the VTM model. Subsequently, this section compares the results from our vehicle models and data collected from the VTM sensor.

2.1 Single-track Model

It is most common to use a single-track model for studying the lateral dynamics of a vehicle [9]. The single-track model (also named the bicycle model) assumes that the tires of the same axle are lumped into one virtual tire. The schematic with dynamics parameters is presented in Figure 2.1. The principal terms and coordinate systems of the vehicle body and wheels are consistent with ISO-8855 [10].

2.1.1 Dynamic Model

The dynamic model has two units, i.e., the tractor and the semi-trailer. Five states are chosen for describing the combination and the state vector x is:

$$x = [v_{x_1},\ v_{y_1},\ \dot{\phi}_1,\ \theta,\ \dot{\theta}], \tag{2.1}$$

where v_{x_1} is the longitudinal speed of the tractor in the tractor local frame, and v_{y_1} is the lateral velocity of CoG of the tractor in the tractor local frame, ϕ_1 is the heading angle (yaw angle) of the tractor in the global frame, $\dot{\phi}_1$ is the yaw rate of the tractor, θ is the articulation angle between the tractor (first unit) and the semi-trailer (second unit), and $\dot{\theta}$ is the rate of change of the articulation angle.

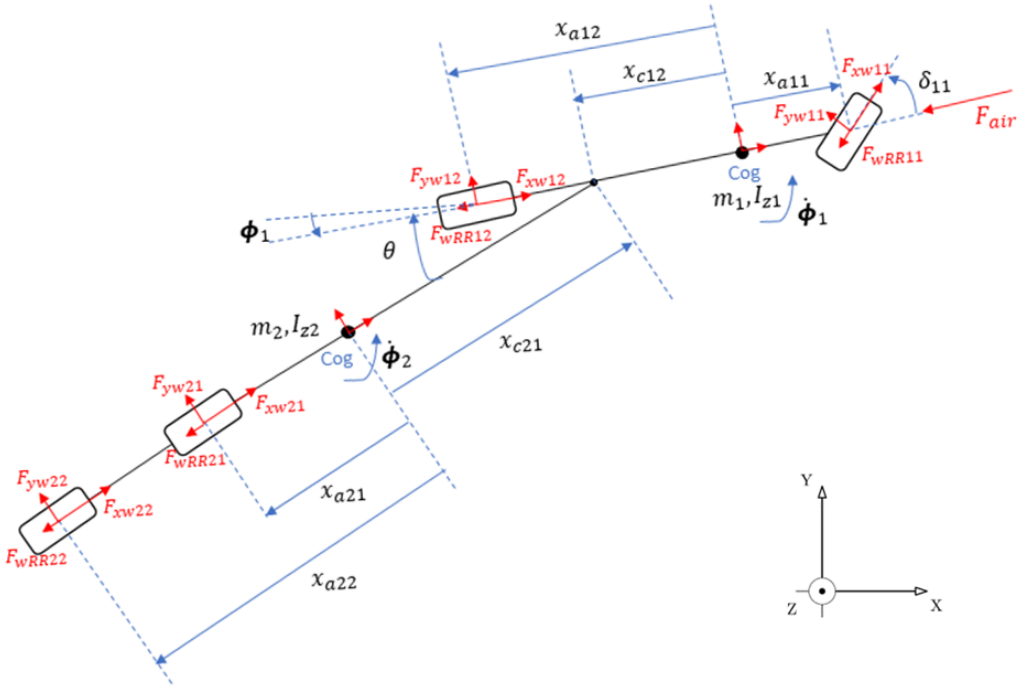

Figure 2.1: Single-track model

Jackknifing occurs due to the loss of lateral force between the tires of the tractor's drive axle and the road surface [11]. To simulate the sudden braking and propelling accurately, the model incorporates longitudinal forces applied to the wheels and the steering angle as inputs. The input vector u is defined as:

$$u = [F_{xw11},\ F_{xw12},\ F_{xw21},\ F_{xw22},\ \delta], \tag{2.2}$$

where δ denotes the steering angle of the tractor's front axle and F_{xwij} denotes the longitudinal force on the virtual lumped wheel. i denotes the unit number, 1 or 2, in this model, and j denotes the axle number, 1 or 2, in each unit. See Figure 2.1.

2.1.2 Lagrangian Equations

A Lagrangian formulation is employed to establish the equations of motion for the dynamics system comprising two units, see e.g. [12]. The Lagrangian equations of the two-unit system are defined as follows:

$$\frac{\mathrm{d}}{\mathrm{d}t} \cdot \frac{\partial T_{kinetic}}{\partial \dot{q_{nc}}} - \frac{\partial T_{kinetic}}{\partial q_{nc}} + \frac{\partial V}{\partial q_{nc}} = Q_{nc}, \quad nc = 1, ..., 4 \tag{2.3}$$

where $T_{kinetic}$ denotes the system's kinetic energy, V denotes the system's potential energy and Q are the generalized forces. q is the generalized coordinates used to describe the position and orientations of the tractor and semi-trailer, nc is the number of generalized coordinates. The generalized coordinates are chosen as follows:

$$q = [X_1,\ Y_1,\ \phi_1,\ \theta], \tag{2.4}$$

where X_1 and Y_1 denote the position of the tractor's CoG on the yaw plane in the global coordinate system. The velocities in the state vector are expressed in the tractor's local frame, and the relationship between the global coordinate and the tractor's local frame can be determined using:

$$\begin{bmatrix} v_{x1} \\ v_{y1} \end{bmatrix} = \begin{bmatrix} \cos(\phi_1) & \sin(\phi_1) \\ -\sin(\phi_1) & \cos(\phi_1) \end{bmatrix} \cdot \begin{bmatrix} \dot{X}_1 \\ \dot{Y}_1 \end{bmatrix} = \begin{bmatrix} \cos(\phi_1) & \sin(\phi_1) \\ -\sin(\phi_1) & \cos(\phi_1) \end{bmatrix} \cdot \begin{bmatrix} v_{X1} \\ v_{Y1} \end{bmatrix}. \tag{2.5}$$

To simplify the parameter symbols, let $v_{X1},\ v_{Y1}$ denote $\dot{X}_1,\ \dot{Y}_1$.

The position of the semi-trailer's CoG in the global coordinate can be calculated by:

$$\begin{bmatrix} X_2 \\ Y_2 \end{bmatrix} = \begin{bmatrix} X_1 \\ Y_1 \end{bmatrix} + \begin{bmatrix} x_{c12}\cos(\phi_1) - x_{c21}\cos(\phi_2) \\ x_{c12}\sin(\phi_1) - x_{c21}\sin(\phi_2) \end{bmatrix}, \tag{2.6}$$

where the yaw angle of the semi-trailer, ϕ_2, can be replaced by:

$$\phi_2 = \phi_1 - \theta. \tag{2.7}$$

The position of the wheels on the same axle in the global coordinate can be represented as:

$$\begin{bmatrix} X_{wij} \\ Y_{wij} \end{bmatrix} = \begin{bmatrix} X_i \\ Y_i \end{bmatrix} + \begin{bmatrix} \cos(\phi_i) \\ \sin(\phi_i) \end{bmatrix} \cdot x_{aij}. \tag{2.8}$$

The global velocity of each wheel can be obtained by taking the time derivative with respect to the wheel's position:

$$v_{Xwij} = \frac{dX_{wij}}{dt} \tag{2.9}$$

$$v_{Ywij} = \frac{dY_{wij}}{dt}. \tag{2.10}$$

The velocity of each wheel in the local coordinate system can be expressed as follows:

$$\begin{bmatrix} v_{xwij} \\ v_{ywij} \end{bmatrix} = \begin{bmatrix} \cos(\phi_i + \delta_{ij}) & \sin(\phi_i + \delta_{ij}) \\ -\sin(\phi_i + \delta_{ij}) & \cos(\phi_i + \delta_{ij}) \end{bmatrix} \begin{bmatrix} v_{Xwij} \\ v_{Ywij} \end{bmatrix}, \tag{2.11}$$

where δ_{11} represents the steering angle of the tractor front axle, while δ_{ij} for other axles are all set to 0, as no steering is possible. Therefore, it is sufficient for the chosen generalized coordinates to describe the motion of the two-unit system [13].

2.1.2.1 Kinetic Energy

The potential energy (V) is zero as the tractor-semi-trailer operates in the level plane. The total kinetic energy $T_{kinetic}$ is the sum of the individual kinetic energies of the tractor and the semi-trailer:

$$T_{kinetic} = \frac{1}{2}(m_1\bar{v}_1^2 + m_2\bar{v}_2^2 + J_1 \cdot \dot{\phi}_1^2 + J_2 \cdot \dot{\phi}_2^2), \tag{2.12}$$

where

$$\bar{v}_1^2 = v_{x1}^2 + v_{y1}^2 \tag{2.13}$$

$$\bar{v}_2^2 = v_{x2}^2 + v_{y2}^2. \tag{2.14}$$

2.1.2.2 Generalized Forces

The generalized forces are defined as:

$$Q_{nc} = \sum_{nk=1}^{n_f} (F_{X_{nk}} \cdot \frac{\partial p_{nk}}{\partial q_{nc}} + F_{Y_{nk}} \cdot \frac{\partial p_{nk}}{\partial q_{nc}}). \tag{2.15}$$

where $F_{X_{nk}}$, $F_{Y_{nk}}$ are the nk^{th} forces element acting on the vehicle units in global coordinates, p_k are the position vectors that describe where force elements act on. The total number of forces in the system is n_f. Those forces are composed of the tire's longitudinal forces F_{xwij} and lateral forces F_{ywij}, and air resistance F_{xair}.

In our motion model, the tires' longitudinal forces F_{xwij} are the input to the system that will cause acceleration or braking. The lateral forces F_{ywij} are calculated by the tire model, which will be introduced in Section 2.3.

The air resistance acting on the tractor's front cross section is given in the tractor's local coordinate frame as

$$F_{xair} = -0.5 \cdot A_f \cdot c_d \cdot \rho_{air} \cdot v_{x1}^2 \frac{v_{x1}}{|v_{x1}|}. \tag{2.16}$$

It is assumed that air resistance force acts on the position of the virtual lumped front axle of the tractor. The translation of air resistance force between the tractor's local coordinate and global coordinate is

$$\begin{bmatrix} F_{Xair} \\ F_{Yair} \end{bmatrix} = \begin{bmatrix} \cos(\phi_1) & -\sin(\phi_1) \\ \sin(\phi_1) & \cos(\phi_1) \end{bmatrix} \cdot \begin{bmatrix} F_{xair} \\ 0 \end{bmatrix} \tag{2.17}$$

2.2 Two-track Model with Load Transfer

During a vehicle's lateral motion, the vehicle's COG is shifted. This leads to transferred vertical weight from the inner wheels to the outer wheels. The vertical load distribution caused by the turning maneuver changes the characteristics of the tire, subsequently affecting the grip generated by the tire model. Consequently, the grip impacts the truck's yaw motion. The single-track model cannot consider the effect of load transfer since the inner and outer wheels are lumped, and thus a two-track model is needed. The two-track model uses Newton's method and considers lateral and longitudinal load transfer.

2.2.1 Kinematic Equations of Two-track Model

Based on the notation in Figure 2.2 and 2.3, the motion equations of the tractor and the semitrailer can be derived as:

$$\begin{aligned} \dot{v}_{x1} = (&F_{xw11l} \cdot \cos\delta + F_{xw11r} \cdot \cos\delta - F_{yw11l} \cdot \sin\delta \\ &- F_{yw11r} \cdot \sin\delta + F_{xw12r} + F_{xw12l} + F_{v1cx} + F_{xair})/m_1 + v_{y1} \cdot \dot{\phi}_1 \end{aligned} \tag{2.18}$$

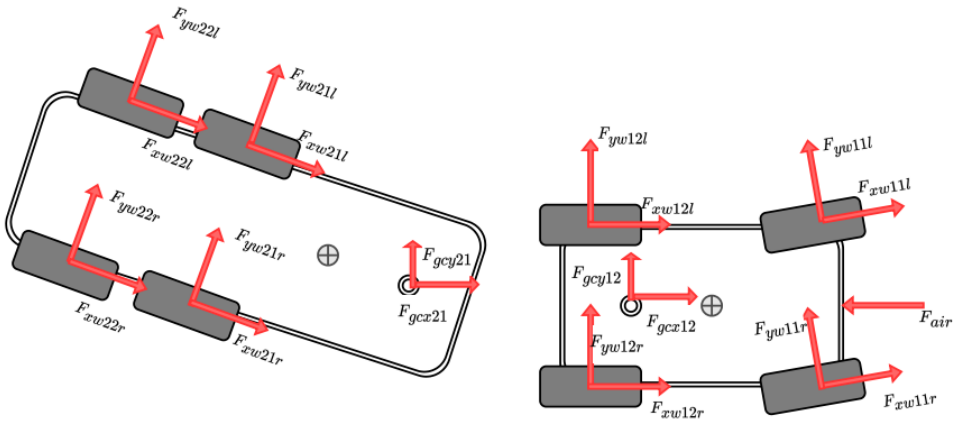

Figure 2.2: Two-track model force

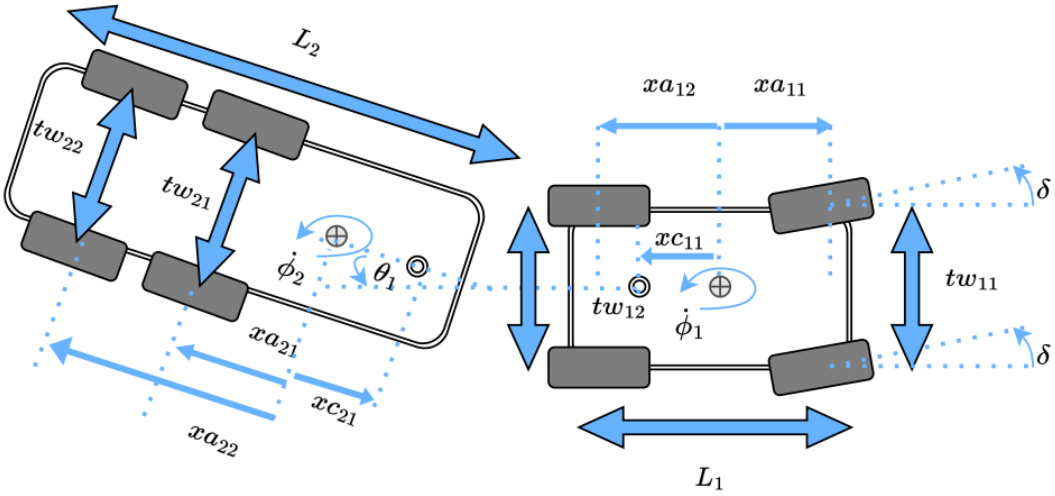

Figure 2.3: Two-track model spacial parameters

$$\dot{v}_{y1} = (F_{xw11l} \cdot \sin\delta + F_{xw11r} \cdot \sin\delta + F_{yw11l} \cdot \cos\delta + F_{yw11r} \cdot \cos\delta + F_{yw12r} + F_{yw12l} + F_{v1cy})/m_1 - v_{x1} \cdot \dot{\phi}_1 \quad (2.19)$$

$$\ddot{\phi}_1 = [xa_{11} \cdot (F_{xw11l} \cdot \sin\delta + F_{xw11r} \cdot \sin\delta + F_{yw11l} \cdot \cos\delta + F_{yw11r} \cdot \cos\delta) + \frac{1}{2}tw_{11} \cdot (-F_{xw11l} \cdot \cos\delta + F_{xw11r} \cdot \cos\delta + F_{yw11l} \cdot \sin\delta - F_{yw11r} \cdot \sin\delta) + xa_{12} \cdot (F_{yw12l} + F_{yw12r}) + \frac{1}{2}tw_{12} \cdot (-F_{xw12l} + F_{xw12r}) + xc_{12} \cdot F_{v2cy}]/Iz_1 \quad (2.20)$$

$$\dot{v}_{x2} = (F_{xw21l} + F_{xw21r} + F_{xw21l} + F_{xw22r} + F_{v2cx})/m_2 + v_{y2} \cdot \dot{\phi}_2 \quad (2.21)$$

$$\dot{v}_{y2} = (F_{yw21l} + F_{yw21r} + F_{yw22l} + F_{yw22r} + F_{v2cy})/m_2 - v_{x2} \cdot \dot{\phi}_2 \quad (2.22)$$

$$\ddot{\phi}_2 = [xa_{21} \cdot (F_{yw21l} + F_{yw21r}) + \frac{1}{2}tw_{21} \cdot (-F_{xw21l} + F_{xw21r}) + xa_{22} \cdot (-F_{xw22l} + F_{xw22r}) + \frac{1}{2}tw_{22} \cdot (-F_{xw22l} + F_{xw22r}) + xc_{21} \cdot F_{v2cy}]/Iz_2 \quad (2.23)$$

The coupling torque around the coupling point where the tractor and trailer connect is considered negligible, meaning the local coupling force on the tractor equals:

$$\begin{bmatrix} F_{v1cx} \\ F_{v1cy} \\ 0 \end{bmatrix} = \begin{bmatrix} \cos(\phi_1) & \sin(\phi_1) & 0 \\ -\sin(\phi_1) & \cos(\phi_1) & 0 \\ 0 & 0 & 1 \end{bmatrix} \cdot \begin{bmatrix} F_{gcx12} \\ F_{gcy12} \\ 0 \end{bmatrix} \quad (2.24)$$

$$\begin{bmatrix} F_{v2cx} \\ F_{v2cy} \\ 0 \end{bmatrix} = \begin{bmatrix} \cos(\phi_2) & \sin(\phi_2) & 0 \\ -\sin(\phi_2) & \cos(\phi_2) & 0 \\ 0 & 0 & 1 \end{bmatrix} \cdot \begin{bmatrix} F_{gcx21} \\ F_{gcy21} \\ 0 \end{bmatrix} \quad (2.25)$$

and the coupling forces from tractor to trailer and from trailer to tractor have the same magnitude but are in opposite directions:

$$F_{gcx12} = -F_{gcx21} \quad (2.26)$$

$$F_{gcy12} = -F_{gcy21} \quad (2.27)$$

2.2.2 Longitudinal Load Transfer

The longitudinal and lateral load transfer is decoupled from each other to make the computations simpler. To simplify the model, several assumptions are made in the methodology of calculating the load transfer. Firstly, the articulation angle between the tractor and trailer is assumed to be small ($\theta \approx 0$). Secondly, the net torque around the pitch axis is zero, and the net vertical force is also zero, which means there is no acceleration in the vertical direction. Thirdly, the left and right wheels on the same axle are assumed to bear identical static vertical loads and experience the same longitudinal load transfer. Lastly, the longitudinal acceleration of trailer a_{x2} approximates the longitudinal acceleration of tractor a_{x1} ($a_{x2} \approx a_{x1}$). Using the

notation defined in Figure 2.4, and the assumptions, the following equilibrium can be obtained:

$$-xa_{11} \cdot F_{z11} - xa_{12} \cdot F_{z12} + (h_1 - h_{c12}) \cdot F_{cx21} + F_{cz21} \cdot xc_{12} = \sum h_1 \cdot F_{xwTractor} \quad (2.28)$$

$$F_{z11} + F_{z12} - F_{cz21} = m_1 \cdot g \quad (2.29)$$

$$F_{cx21} = m_2 \cdot a_{x1} - F_{xwg2} \quad (2.30)$$

$$(h_{c21} - h_2) \cdot F_{cx21} - xc_{21} \cdot F_{cz21} - xa_{g2} \cdot F_{zg2} = h_2 \cdot F_{zwg2} \quad (2.31)$$

$$F_{cz21} + F_{zg2} = m_2 \cdot g \quad (2.32)$$

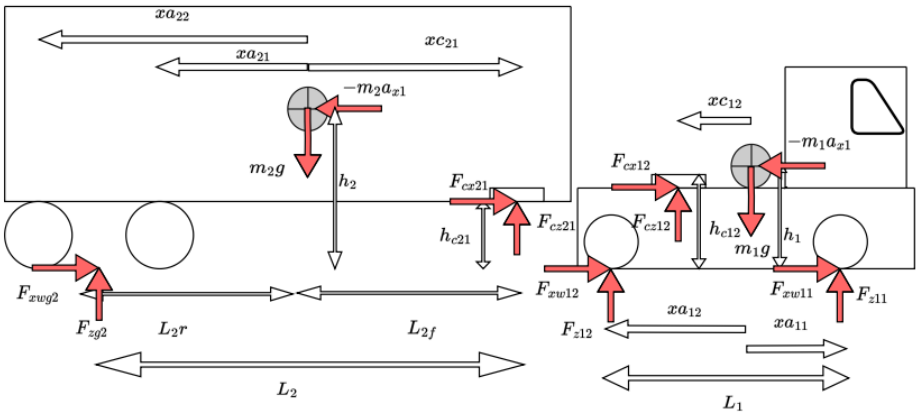

Figure 2.4: Parameters for calculating load transfer

As this is a linear system of equations, the vertical force on each axle can be obtained by solving the inverse function:

$$AF = b \quad (2.33)$$

with F being the vertical load:

$$F = \begin{bmatrix} F_{z11} & F_{z12} & F_{cx21} & F_{cz21} & F_{zg2} \end{bmatrix}^\intercal \quad (2.34)$$

and A and b derived from Equation 2.28-2.32 as:

$$A = \begin{bmatrix} -xa_{11} & -xa_{12} & h_1 - h_{c12} & xc_{12} & 0 \\ 1 & 1 & 0 & -1 & 0 \\ 0 & 0 & 1 & 0 & 0 \\ 0 & 0 & hc_{21} - h_2 & -xc_{21} & -0.5(xa_{21} + xa_{22}) \\ 0 & 0 & 0 & 1 & 1 \end{bmatrix} \quad (2.35)$$

$$b = \begin{bmatrix} h_1 \cdot (F_{xw11l} + F_{xw12l} + F_{xw11r} + F_{xw12r}) \\ m_1 \cdot g \\ m_2 \cdot a_{x1} - F_{xw21l} - F_{xw22l} - F_{xw21r} - F_{xw22r} \\ h_2 \cdot (F_{xw21l} + F_{xw22l} + F_{xw21r} + F_{xw22r}) \\ m_2 \cdot g \end{bmatrix} \quad (2.36)$$

The vertical load on the left and right wheels due to gravity and longitudinal load transfer can then be found as:

$$F_{z11l} = F_{z11r} = \frac{1}{2}F_{z11} \tag{2.37}$$

$$F_{z12l} = F_{z12r} = \frac{1}{2}F_{z12} \tag{2.38}$$

$$F_{z21l} = F_{z21r} = F_{z22l} = F_{z22r} = \frac{1}{4}F_{zg2} \tag{2.39}$$

2.2.3 Lateral Load Transfer

The amount of lateral load transfer on the tractor's front axle due to the shift of the tractor's CoG is defined as:

$$F_{lat_{11}} = m_1 \cdot a_{y1} \cdot \left(\frac{hr_{11} \cdot (-xa_{12})}{L_1 \cdot tw_{11}} + \frac{\Delta h \cdot cr_{11}}{tw_{11} \cdot (cr_{11} + cr_{12})} \right) \tag{2.40}$$

For the tractor rear axle:

$$F_{lat_{12}} = m_1 \cdot a_{y1} \cdot \left(\frac{hr_{12} \cdot xa_{11}}{L_1 \cdot tw_{12}} + \frac{\Delta h \cdot cr_{12}}{tw_{12} \cdot (cr_{11} + cr_{12})} \right) \tag{2.41}$$

where hr_{ij} is the height of the axle roll center, cr_{ij} is the axle's roll stiffness, L_i is the length of the wheelbase of i unit. The parameter to calculate the lateral load transfer due to suspension compliance can be computed as follows:

$$\Delta h = h_1 - \frac{-xa_{12} \cdot hr_{11} + xa_{11} \cdot hr_{12}}{L_1}.$$

The two axles of the trailer are grouped into a single axle to calculate the load transfer of the trailer:

$$L_{2r} = -\frac{xa_{21} + xa_{22}}{2} \tag{2.42}$$

$$L_{2f} = xc_{21} \tag{2.43}$$

$$L_2 = L_{2r} + L_{2f} \tag{2.44}$$

$$F_{lat_{2c}} = m_2 \cdot a_{y2} \cdot \frac{h_2 \cdot L_{2r}}{L_2 \cdot tw_2} \tag{2.45}$$

$$F_{lat_2} = m_2 \cdot a_{y2} \cdot \frac{h_2 \cdot L_{2f}}{L_2 \cdot tw_2} \tag{2.46}$$

where $hr_{g2} = \frac{1}{2}hr_{21} + \frac{1}{2}hr_{22}$ is the trailer's axle-group roll center height, $cr_{g2} = cr_{21} + cr_{22}$ is the trailers' axle-group roll stiffness. The track width of the trailer tw_{g2} equals the mean of the tw_{21} and tw_{22}. The suspension of the trailer is ignored in this calculation to simplify the model.

In addition to the load transfer caused by the shift of the tractor's CoG, it is assumed that the tractor rear axle experiences lateral load transfer due to the shift of the

trailer's CoG through the coupling. However, considering the substantial distance from the tractor front axle to the coupling point, the computation is simplified by assuming that the load transfer from the trailer has no impact on the vertical load on the tractor front axle, leading to:

$$\begin{aligned}
F_{Z11r} &= F_{z11r} + F_{lat_{11}} \\
F_{Z11l} &= F_{z11l} - F_{lat_{11}} \\
F_{Z12r} &= F_{z12r} + F_{lat_{11}} + F_{lat_{2c}} \\
F_{Z12l} &= F_{z12l} - F_{lat_{11}} - F_{lat_{2c}} \\
F_{Z21r} &= F_{z21r} + \frac{1}{2}F_{lat_2} \\
F_{Z21l} &= F_{z21l} - \frac{1}{2}F_{lat_2} \\
F_{Z22r} &= F_{z22r} + \frac{1}{2}F_{lat_2} \\
F_{Z22l} &= F_{z22l} - \frac{1}{2}F_{lat_2}
\end{aligned} \tag{2.47}$$

2.3 Tire Model

The selection of the tire model is a balance between complexity and accuracy. A too-complex model is a computationally expensive choice when driving the simulation in real time.

2.3.1 Pure Lateral Slip Model

Unlike passenger car tires, the correlation between tire cornering stiffness and vertical load is almost linear for truck tires [14]. The pure linear slip model assumes the longitudinal slip is small, the tire's lateral force F_{ywijk} is proportional to the lateral slip s_y as:

$$F_{ywijk} = -c_{yijk} \cdot s_{yijk} \tag{2.48}$$

$$s_{yijk} = \frac{v_{wyijk}}{|v_{wxijk}|}, \tag{2.49}$$

where c_{yijk} is the normalized equivalent cornering stiffness, which is calculated by dividing the tire cornering stiffness by its vertical load, and s_{yijk} represents the lateral slip of each wheel, v_{wxijk} and v_{wyijk} indicate the local velocity of the particular wheel in the x and y directions.

In reality, the tire cannot produce a lateral force exceeding the friction limit ($\mu \cdot F_z$). To handle this problem, a hyperbolic tire model is proposed and used:

$$F_{ywijk} = \mu \cdot F_{Zijk} \cdot \tanh\left(\frac{-c_{yijk} \cdot s_{yijk}}{\mu}\right). \tag{2.50}$$

The hyperbolic tire model offers a closer approximation to the lateral force generated by the linear tire model when the lateral slip magnitude is small. Moreover, it incorporates the concept of setting a friction limit for both high and low thresholds of lateral slip because the tanh term in the equation ranges from -1 to 1, which means the lateral force of the wheels varies from $-\mu \cdot F_{Zijk}$ to $\mu \cdot F_{Zijk}$.

During turning, vehicles counteract centrifugal and inertial forces with the tire's lateral forces (grip forces) for directional stability, and jackknifing would arise from grip loss. The loss of lateral grip would occur when one operates the vehicle combining cornering with braking or propulsion due to the excessive wheel torque [15].

When jackknifing happens, it is common for the longitudinal slip s_x and lateral slip s_y components of the braking tire to become significant. It is crucial to consider the effect of these high slip values when determining the magnitude of the lateral forces. The pure lateral slip model's inaccuracy lies in its assumption of zero longitudinal slip. However, in real-world scenarios, the pure lateral slip model holds only when the absolute value of the wheel's longitudinal slip remains low. In high longitudinal slip instances, an increase in longitudinal slip leads to a reduction in the lateral force exerted by the wheel. The pure lateral slip model's accuracy falls short in effectively portraying the lateral forces on the wheels, and it inadequately represents the vehicle's dynamics.

2.3.2 Combined Slip Model

A combined slip model can be used to capture both lateral and longitudinal slip. This model makes it possible to capture vehicle instabilities like jack-knifing better. The longitudinal slip is defined as:

$$s_x = -\frac{v_{wx} - R \cdot \omega}{v_{wx}}, \tag{2.51}$$

where R is rolling radius and ω is the angular speed of the rolling wheel. The longitudinal slip is a key factor for determining the longitudinal force's magnitude. The single-track and the two-track models use the longitudinal forces of each axle as input variables F_x instead of the longitudinal slips s_x to simplify the modeling. With F_x as the input variable, the effect of combined slip can be described by multiplying the lateral force under zero longitudinal slip and a weighting factor:

$$F_{ywijk} = \underbrace{\sqrt{1 - (\frac{F_{xwijk}}{e\mu F_{Zijk}})^2}}_{\Phi_{xijk}} \cdot F_{ywijk}|_{(s_x=0)}. \tag{2.52}$$

In the single-track model, F_{Zijk} represents the static vertical load on the wheels, while in the two-track model, it stands for the vertical load on each wheel considering load transfer effects.

The lateral force when longitudinal slip is zero, i.e. $F_{ywijk}|_{(s_{xijk}=0)}$ is given by Equation 2.50. When it comes to combined lateral force, in Equation 2.50, pure lateral

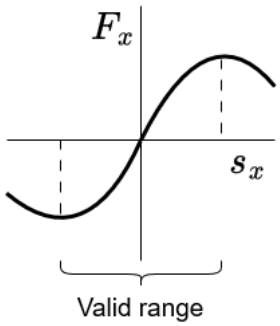

Figure 2.5: Valid range of s_x within F_x vs. s_x curve when employing F_x as input variable

slip s_{yijk} is replaced by the equivalent slip angle $s_{yijk|eq} = \frac{1}{\Phi_{xijk}} \cdot s_{yijk}$. There comes to:

$$F_{ywijk} = \mu \cdot F_{Zijk} \cdot \tanh\left(\frac{-c_{yijk} \cdot s_{yijk|eq}}{\mu}\right). \tag{2.53}$$

e defines the shape of the friction circle, also called conservativity of the model. When $e = 1$, the shape is a circle. When $e > 1$, the shape is an ellipse. For a smaller value of e, the upper limit lateral force is lower, which means the tire model is more conservative. Conversely, the higher e, the less conservative the tire model is.

The objective of the combined slip model using F_x as an input is to simulate a scenario where, as the longitudinal force F_x increases, the corresponding lateral force diminishes. However, in reality, there are instances where, with large longitudinal slip s_x, the wheel provides insufficient lateral force F_y even when the longitudinal force F_x is small. This situation the combined slip model using F_x can not effectively represent the dynamics of the wheel. Therefore, an inherent limitation of using F_x as an input variable is that, although s_x is excluded in the system, the F_x vs s_x curves should show a positive slope over the entire range of s_x except when the wheel is lock ($F_x = \mu \cdot F_Z$). Failure to limit the range of s_x implies the model is only valid within the region between the two peaks of F_x vs. s_x curves. In this way, it is ascertained that F_y vs. F_x curves have a unique value when employing F_x [16]. This combined slip model indicates that the modeled vehicle requires a slip controller to restrain s_x to maintain the modeling validity.
In the global system, the tire forces are

$$\begin{bmatrix} F_{Xijk} \\ F_{Yijk} \end{bmatrix} = \begin{bmatrix} \cos(\phi_i + \delta) & -\sin(\phi_i + \delta) \\ \sin(\phi_i + \delta) & \cos(\phi_i + \delta) \end{bmatrix} \cdot \begin{bmatrix} F_{xwijk} \\ F_{ywijk} \end{bmatrix}, \tag{2.54}$$

where $\delta = 0$ if the axle is a non-steerable axle.

2.3.3 Calculation for Lateral Tire Slip of One-track Model and Two-track Model

Both the single-track model and the two-track model use a friction circle-inspired combined slip model as described above. To obtain the lateral slip s_{yijk}, the local

velocities of the wheel in X and Y directions are needed according to Equation 2.49.

For the single-track model, the local velocity of a particular wheel is directly calculated by Equation 2.11. However, in the two-track model, the calculation of lateral slip differs because the left and right wheels have different positions and velocities. The position of the wheels can be determined as:

$$\begin{bmatrix} X_{wijr} \\ Y_{wijr} \end{bmatrix} = \begin{bmatrix} X_i \\ Y_i \end{bmatrix} + \begin{bmatrix} \cos(\phi_i) & -\sin(\phi_i) \\ \sin(\phi_i) & \cos(\phi_i) \end{bmatrix} \cdot \begin{bmatrix} xa_{ij} \\ -\frac{tw_{ij}}{2} \end{bmatrix} \tag{2.55}$$

and

$$\begin{bmatrix} X_{wijl} \\ Y_{wijl} \end{bmatrix} = \begin{bmatrix} X_i \\ Y_i \end{bmatrix} + \begin{bmatrix} \cos(\phi_i) & -\sin(\phi_i) \\ \sin(\phi_i) & \cos(\phi_i) \end{bmatrix} \cdot \begin{bmatrix} xa_{ij} \\ \frac{tw_{ij}}{2} \end{bmatrix} \tag{2.56}$$

The global velocity of the wheels is obtained by differentiating the position with respect to time.

$$v_{Xwijk} = \frac{dX_{wijk}}{dt} \tag{2.57}$$

$$v_{Ywijk} = \frac{dY_{wijk}}{dt} \tag{2.58}$$

Here, the index k can be either "l" for the left wheel or "r" for the right wheel.

The local velocity of the wheels can be calculated by transforming the global velocity to the wheels' local coordinate system:

$$\begin{bmatrix} v_{xwijk} \\ v_{ywijk} \end{bmatrix} = \begin{bmatrix} \cos(\phi_i + \delta_{ij}) & \sin(\phi_i + \delta_{ij}) \\ -\sin(\phi_i + \delta_{ij}) & \cos(\phi_i + \delta_{ij}) \end{bmatrix} \cdot \begin{bmatrix} v_{Xwijk} \\ v_{Ywijk} \end{bmatrix} \tag{2.59}$$

Finally, the lateral slip of each wheel is given by:

$$s_{yijk} = \frac{v_{ywijk}}{|v_{xwijk}|} \tag{2.60}$$

2.4 High Fidelity Model and Preconditions for Validation

Vehicle motion prediction relies on a dynamic model, and the accuracy of this model is crucial for motion prediction. Several tests were done with both our models and a high-fidelity model to examine the accuracy of the dynamic models. Preconditions and vehicle parameters are the same in those two models.

2.4.1 High Fidelity Model: VTM

VTM is an abbreviation of Volvo Transport Model developed by Volvo Group Trucks Technology (GTT), which minimizes MBS (multi-body system) bodies as many as possible but still satisfies to represent vehicle dynamics in steady and severe

situations [17]. VTM is built in MATLAB/Simulink, including chassis, wheels, tires, and suspension. Besides, there are established parameter files for different forms of tractors and trailers. Users can customize the model according to their own studies' requirements. The plant model has sensors that supply the vehicle's motion measurement data. The designed prediction algorithm relies on these sensors for motion prediction. VTM uses PAC2002 [16] as the tire model, which is different from the tire model of our built motion model.

2.4.2 Driver Model

A driver model is utilized to mimic driver behavior. The driver model comprises two subsystems: speed controller and path follower. In the validation and simulation, only the speed controller is used.

2.4.2.1 Speed Controller

The speed controller tries to maintain the vehicle speed by changing the longitudinal wheel forces. The speed controller is a PI-controller [18]:

$$F_x^{driver} = (K_p + K_i \cdot \frac{1}{s}) \cdot (v_x^{ref} - v_x), \tag{2.61}$$

where K_p is the proportional gain that equals 1×10^5 and K_i is the integral gain that equals 1×10^4. The input is the error between the reference speed v_x^{ref} and the current tractor's longitudinal speed v_{x1}. The output from the speed controller is the total longitudinal force F_x^{driver} on the driven axle.

2.4.3 Actuator Modeling

The torque generated by the electric motor, the actuator in the e, does not instantaneously attain the requested torque value. The motor's response is modeled as a low-pass filter to simulate its reaction to the request torque, specifically capturing the time delay characteristics.

$$G_{act}(s) = \frac{1}{\tau_{act} \cdot s + 1} \tag{2.62}$$

where τ_{act} is the time constant. In this work, the time constant is 0.2 s.

In addition, it is assumed that the requested force for each actuator must not exceed the friction limit on the corresponding wheel. The constraint is applied to avoid the wheels spinning backward:

$$-\mu \cdot F_{Zijk} \cdot r_{ijk} \leq T_{xwijk}^{req} \leq \mu \cdot F_{Zijk} \cdot r_{ijk} \tag{2.63}$$

2.4.4 Brake System

The requested brake force is assumed to remain constant in the vehicle's braking process. In this system, the tractor's front axle is considered a non-powered and

non-braked axle, while the tractor's rear axle is powered and braked. As for the trailer axles, they are considered non-powered and braked. This configuration is made because the studied truck has an electric-powered tractor and a conventional trailer. When we apply a strong braking force on the tractor's powered rear axle, as long as there is no occurrence of jackknifing, the regenerative energy can be maximized.

2.4.4.1 Tractor Rear Axle Brake

Electric vehicles are usually driven using one-pedal drive mode to regenerate as much energy as possible. In this mode, when the driver decides to brake, the requested brake force is exclusively applied to the tractor's rear drive axle to convert mechanical energy to electricity. Nevertheless, relying solely on the braking of the tractor's rear axle increases the probability of experiencing yaw instability. The brake torque is distributed as 50/50 between the left and right sides:

$$T_{xw12l}^{req} = T_{xw12r}^{req} = 0.5T_{TotalReq} \tag{2.64}$$

2.4.4.2 Trailer Brake

Trailer braking can be used to avoid jackknifing. While the total brake force remains unchanged during trailer braking, the distribution of brake forces is altered. Instead of solely applying brake force on the tractor's rear axle, it is now distributed based on the static weight of the tractor's rear axle, the trailer's front axle, and the trailer's rear axle. Furthermore, equal brake torque is applied to the same axle's left and right wheels.

$$br_{ij} = \frac{Fz_{ij}}{Fz_{12}+Fz_{21}+Fz_{22}} \tag{2.65}$$

$$T_{xwijk}^{req} = 0.5T_{TotalReq}br_{ij} \tag{2.66}$$

2.4.5 Slip Controller

A basic ABS is implemented in the VTM model to control the longitudinal slip. The ABS aims to keep the longitudinal slip of the tractor's rear axle wheels and trailer axle wheels within a range of 0.1 to -0.1. This is achieved by adjusting the torque signal sent to the actuator. The ABS calculates the appropriate amount of braking torque based on the feedback from the VTM's longitudinal slip and longitudinal force at the contact patch.

The slip controller helps jackknife prediction because the friction circle-inspired combined slip model utilized in the predictor is more sensitive to the risk of jackknifing when the longitudinal slip is low. This sensitivity arises due to the more pronounced reduction in lateral forces given by the hyperbolic tangent tire model within the predictor when the longitudinal slip is low. In contrast, this reduction in lateral forces is smaller in the Pacejka tire model when the longitudinal slip is low. This leads the predictor to potentially anticipate jackknifing because of the insufficient lateral forces available in these conditions.

2.5 Validating Two Models with VTM

Both the single-track model and the two-track model can exhibit certain dynamic characteristics. These models are frequently used to analyze the yaw motion behavior. However, the single-track and two-track models may not be capable of describing the tractor semi-trailer's yaw motion when jackknifing occurs. The following section aims to validate the accuracy of the single-track and two-track models by comparing the simulation results obtained from the high-fidelity VTM model under several driver maneuvers. The comparison between tractor yaw rate, tractor longitudinal velocity, articulation angle, and jackknife detection threshold is presented in this part.

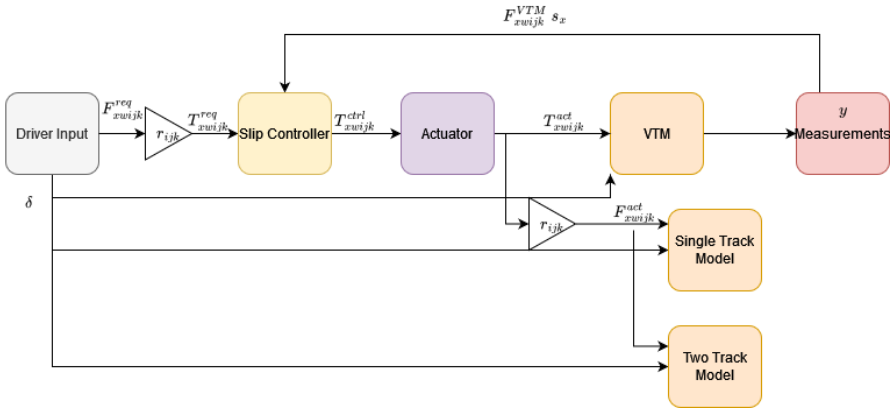

Figure 2.6: Flowchart of Model Validation Process Using VTM.

To validate the models, the same input is used for the proposed models and the VTM model, which is assumed to reflect reality. The process is illustrated in Figure 2.6. The input torque from the driver first passes through the slip controller, which, based on certain measurements, gives T_{xwijk}^{ctrl} to the wheel torque actuator. The wheel torque input for VTM is from the actuator and then divided by the wheel radius to derive the wheel forces. These wheel forces are used as inputs for the two-track model. Furthermore, to obtain the forces on each axle, the forces on the wheel of the same axle are added and used as the input for the single-track model. In the subsequent tests, the road friction coefficient maintains 0.3.

2.5.1 Lane Change

A lane change maneuver is performed by giving a single sinusoidal steering angle input. During the lane change phase, the truck remains at the constant longitudinal speed at 40 km/h, achieved by the speed controller. The slip controller is off when performing lane change maneuvers. Figure 2.7 provides a comparison of the yaw rate difference calculated by Equation 3.12, 3.13, articulation angle, tractor yaw rate, and tractor longitudinal velocity obtained from the single-track model, the two-track model, and the VTM. The simulation is terminated after 15 seconds.

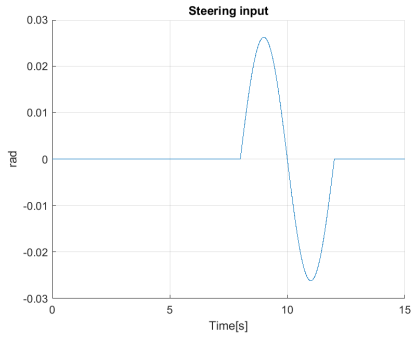

(a) Steering angle input for lane change manoeuvre.

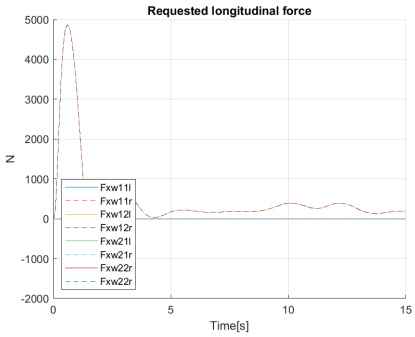

(b) Wheel forces input for lane change manoeuvre.

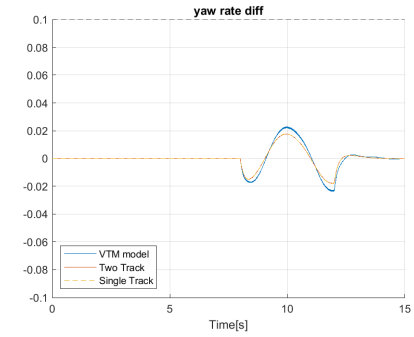

(c) Yaw rate difference $\dot{\phi}_1 - \dot{\phi}_{ref}$.

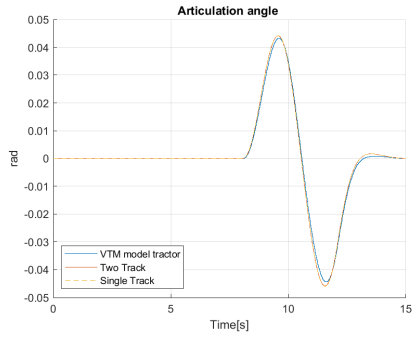

(d) Articulation angle θ.

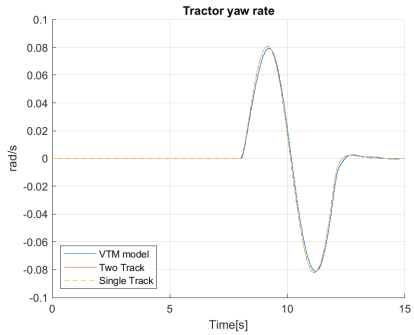

(e) Tractor yaw rate ω_1.

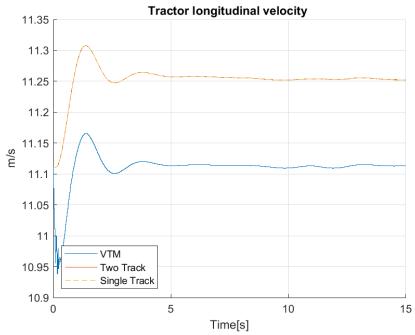

(f) Longitudinal velocity of tractor v_{x1}.

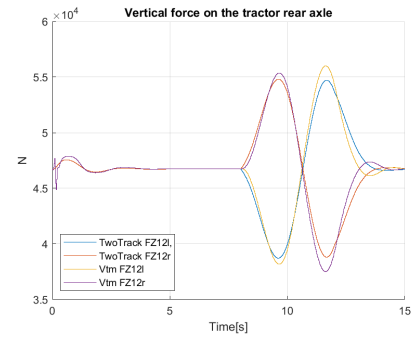

(g) Vertical load on the tractor rear axle.

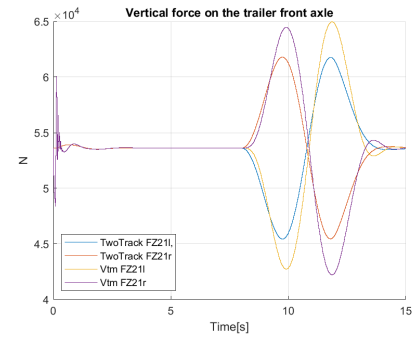

(h) Vertical load on the trailer front axle.

Figure 2.7: Simulation results of the single-track model, the two-track model, and the VTM under the lane change maneuver test at 40 km/h and $\mu = 0.3$ with conservativity $e = 1$.

2.5.2 Steady State Cornering and Braking

In the steady state cornering and braking case, the truck maintains a constant speed of 40 km/h. Before initiating the braking action, the speed controller decides the input torques/longitudinal tire forces. The steering angle input starts increasing at 5s at a steady rate of 0.005 rad/s until reaching 0.0542 rad. This specific steering angle, combined with the constant speed, will yield a cornering circle with a radius of 72 m. After reaching a steady state and at time instant 40s, the requested brake forces are applied in the tractor rear axle.

The above maneuver was used in two cases: one with gentle braking forces and the other with strong braking forces. It is important to note that the requested brake forces may exceed the actual input brake forces, as the slip controller could adjust the brake intensity to avoid excessive longitudinal slip.

The simulation was stopped when either the time reached 60^{th} second or the articulation angle from the VTM ground truth reached $\pi/3$ rad. This articulation angle corresponded to a severe jackknifing under the initial velocity.

2.5.2.1 Gentle Braking

The requested brake force on the tractor rear axle is $-15000N$ and is equally distributed on the left and right wheels. Figure 2.8a and Figure 2.8b depict the driver maneuvers in this case. Figure 2.8 indicates the two-track model captures jackknife. However, the single-track and the VTM suggest the truck is safe.

To ascertain the significant disparity when compared with VTM results from the tire model employed in the two-track model, thus making it more prone to jackknifing, another test is introduced as shown in Figure 2.11. This test raises the conservativity factor to $e = 1.1$ while keeping all other parameters unchanged.

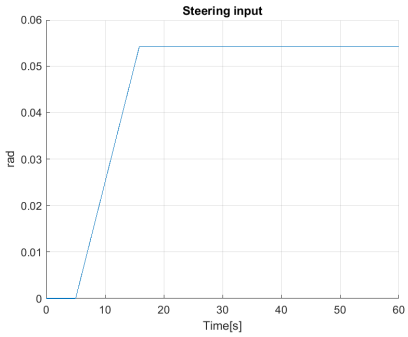

(a) Steering angle input.

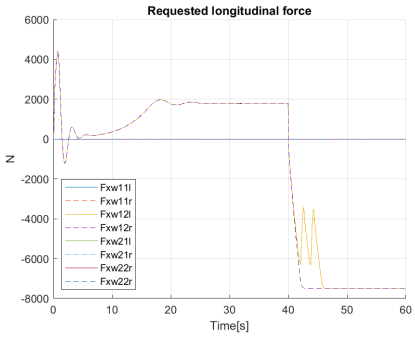

(b) Wheel forces input

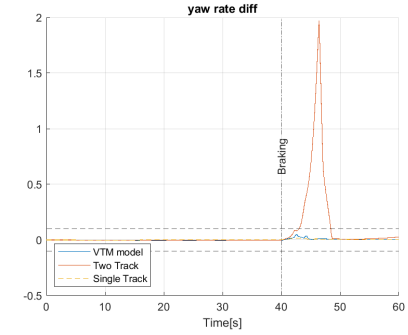

(c) Yaw rate difference $\dot{\phi}_1 - \dot{\phi}_{ref}$.

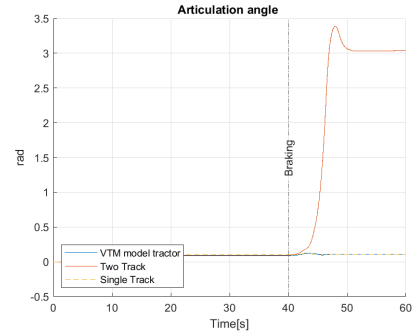

(d) Articulation angle θ.

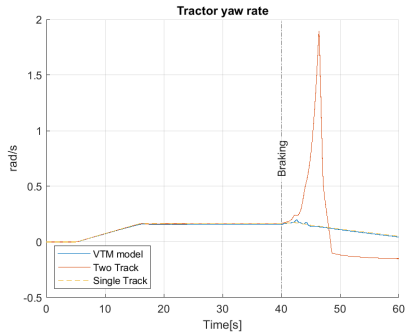

(e) Tractor yaw rate ω_1.

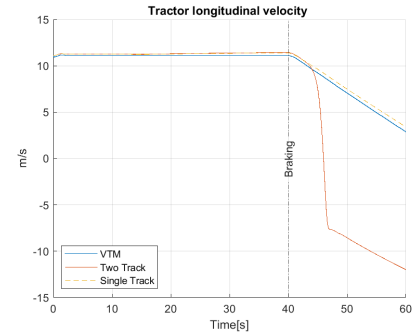

(f) Longitudinal velocity of tractor v_{x1}.

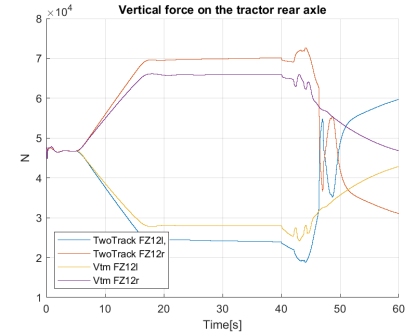

(g) Vertical load on tractor rear axle.

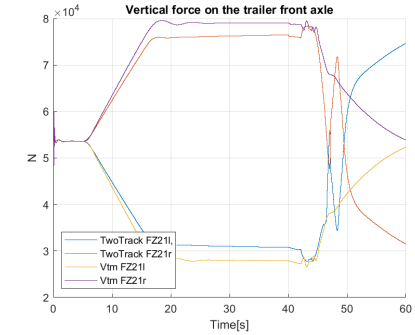

(h) Vertical load on trailer front axle.

Figure 2.8: Simulation results of the single-track model, two-track model, and VTM in cornering and gentle braking test at 40 km/h and $\mu = 0.3$ with conservativity $e = 1$.

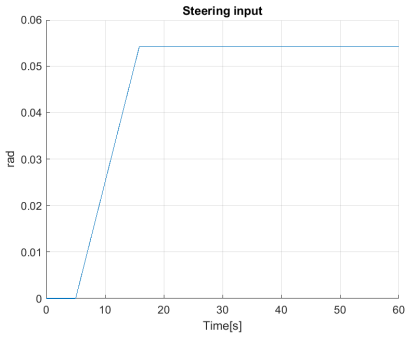

(a) Steering angle input.

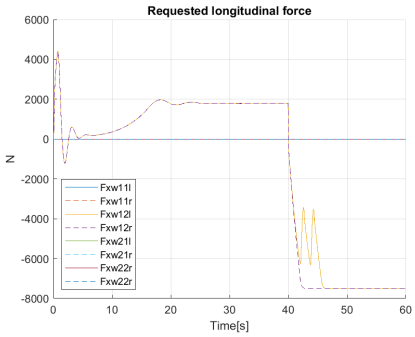

(b) Wheel forces input.

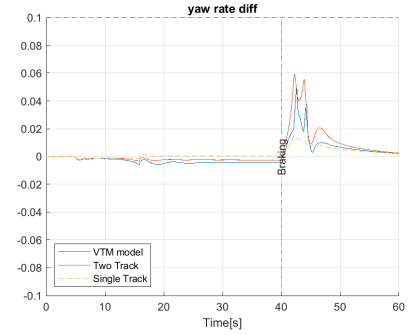

(c) Yaw rate difference $\dot{\phi}_1 - \dot{\phi}_{ref}$.

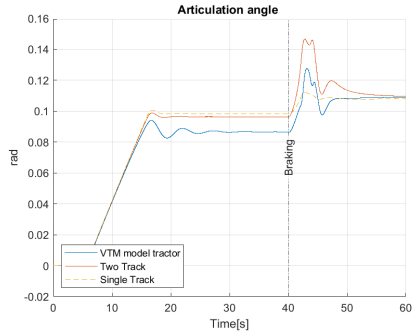

(d) Articulation angle θ.

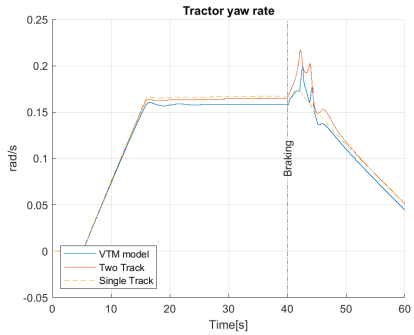

(e) Tractor yaw rate ω_1.

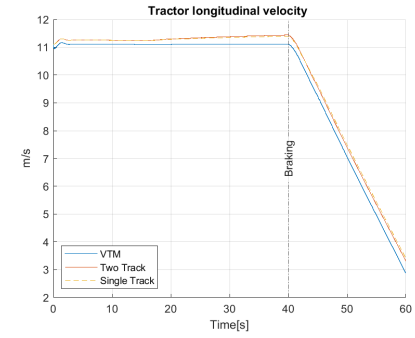

(f) Longitudinal velocity of tractor v_{x1}.

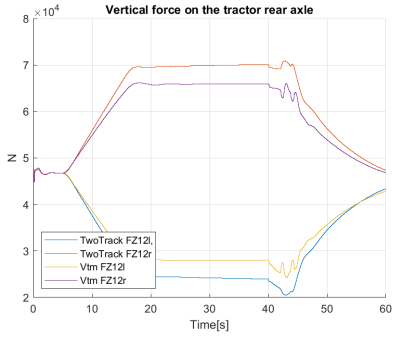

(g) Vertical load on tractor rear axle.

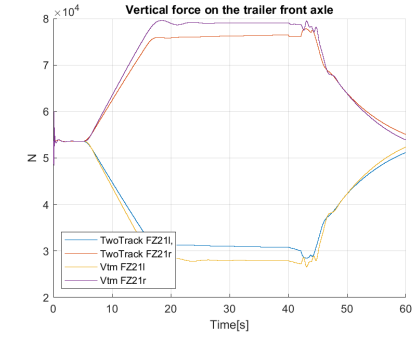

(h) Vertical load on trailer front axle.

Figure 2.9: Simulation results of the single-track model, two-track model, and VTM in cornering and gentle braking test at 40 km/h and $\mu = 0.3$ with increased conservativity $e = 1.1$.

2.5.2.2 Strong Braking and Jackknife

The requested brake force is twice as large as the gentle case, -30000 N. The total mass of the tractor and the trailer is 101810 kg and the approximate intended retardation $a = 0.295\ m/s^2$. Figure 2.10 illustrates the simulation results with a conservativity factor of $e = 1$, while Figure 2.11 shows the simulation results with a conservativity factor of $e = 1.1$. Figure 2.10a and Figure 2.10b show the input to perform the maneuver. By examining Figure 2.10 and Figure 2.11, it can be seen that the occurrence of truck jackknifing in both the two-track model and the VTM. However, according to the simulation results from the single-track model, the truck remains stable.

2.5.3 Performance Evaluation for Single-track and Two-track Model

Results suggest that both the single-track and two-track models capture the specified vehicle's motion under normal driving conditions. The difference in the dynamics described by these models is relatively minor. In the lane change test, both the single-track and two-track models closely align with the results obtained from VTM. Additionally, the two-track model is similar to the VTM concerning the magnitude of vertical loads. A minor discrepancy is observed in the delayed load transfer from the VTM compared to the two-track model, and the amount of load transfer at different wheels does not perfectly match the amount of load transfer obtained by the VTM. Although the difference in roll dynamics is minor, this difference has some impact on the yaw dynamics and furthermore influences the model's ability to capture jackknifing.

However, in extreme driving conditions, the single-track and two-track models have large discrepancies compared with the VTM. The single-track model fails to capture jackknifing. One reason for the failure of the single-track model to capture jackknife is because it lumps the wheel on the same axle and thus assumes the lumped axle was capable of providing the grip. In the VTM and the two-track model, it is believed that the inner wheel can merely provide the lateral force, and thus jackknife will happen. By contrast, the single-track model can not sense the inefficiency in lateral force provided by the inner wheel, leading to the erroneous assumption that the virtual lumped wheel can provide sufficient lateral force.

It can be seen from Figure 2.8 that the two-track model falsely detects the jackknife when the truck brakes in the gentle braking case. Furthermore, while both the two-track model and the VTM exhibit jackknifing events during the strong braking situation, as shown in Figure 2.10, the two-track model exhibits a more severe and earlier jackknifing comparing the actual occurrence of jackknifing in the VTM high fidelity model. The discrepancies mainly arise due to the limitations of the employed tire model in the single-track and two-track models. The Pacejka tire model used in the VTM is more advanced and can better represent real-world scenarios than the tire model used in the single-track and two-track models.

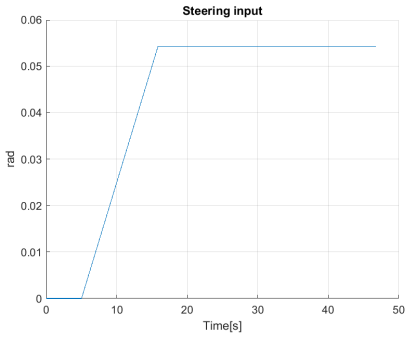

(a) Steering angle input.

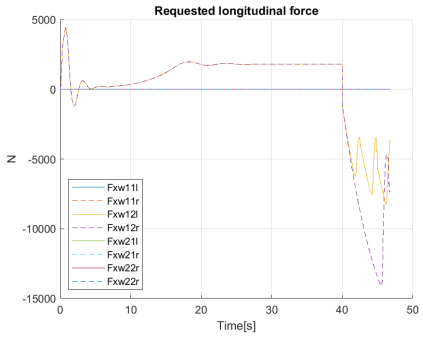

(b) Wheel forces input.

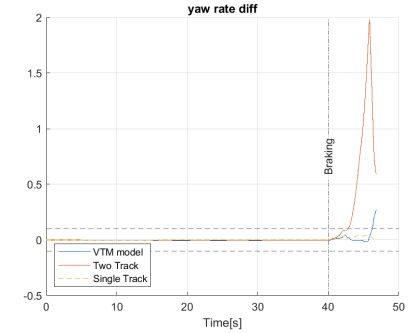

(c) Yaw rate difference.

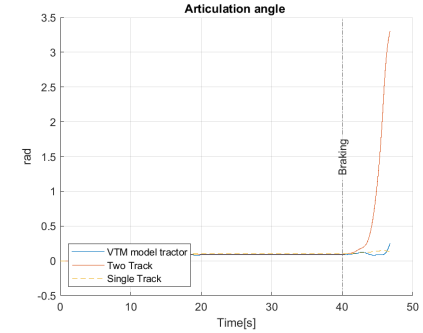

(d) Articulation angle θ.

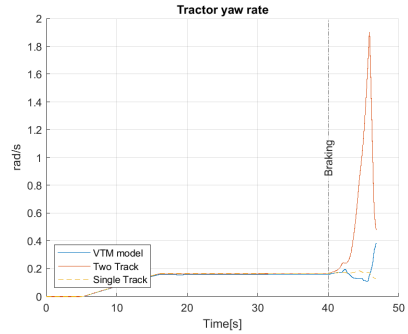

(e) Tractor yaw rate ω_1.

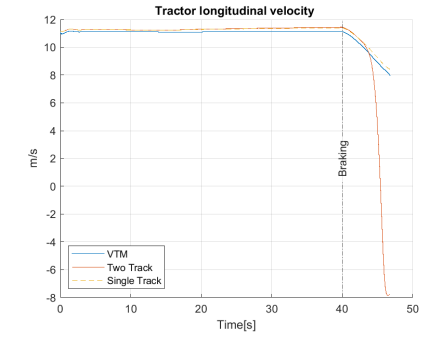

(f) Longitudinal velocity of tractor v_{x1}.

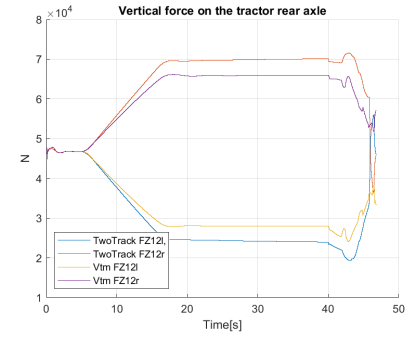

(g) Vertical load on tractor rear axle.

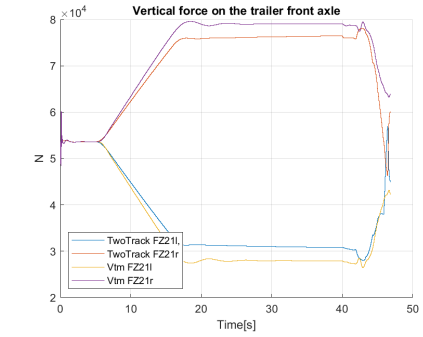

(h) Vertical load on trailer front axle.

Figure 2.10: Simulation results of the single-track model, two-track model, and VTM in cornering and strong braking test at 40 km/h and $\mu = 0.3$ with conservativity $e = 1$

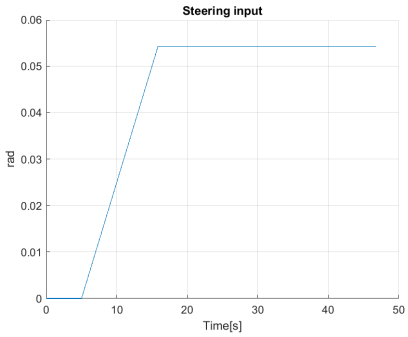

(a) Steering angle input.

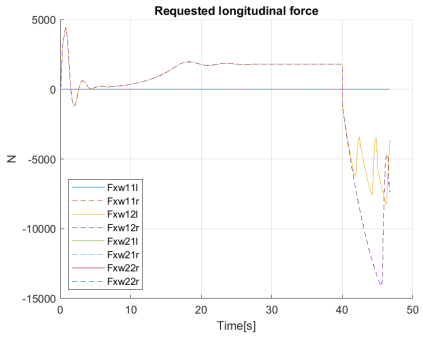

(b) Wheel forces input.

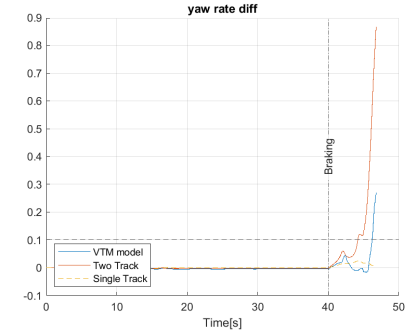

(c) Yaw rate difference.

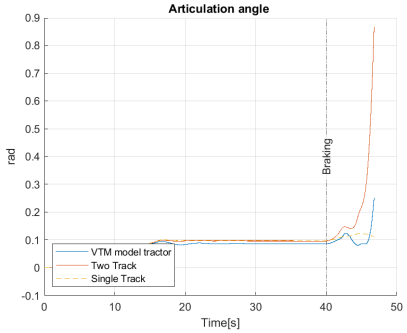

(d) Articulation angle θ.

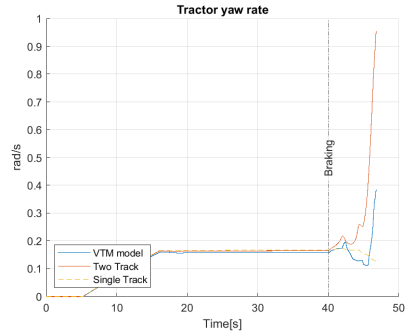

(e) Tractor yaw rate ω_1.

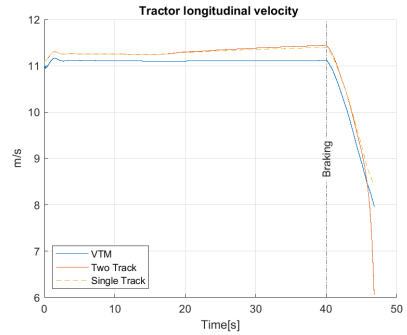

(f) Longitudinal velocity of tractor v_{x1}.

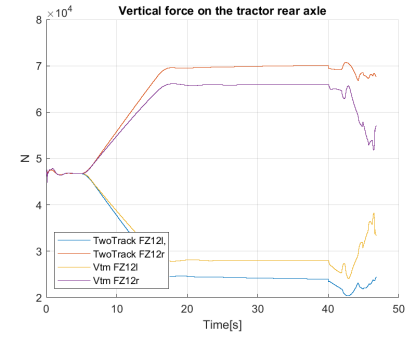

(g) Vertical load on tractor rear axle.

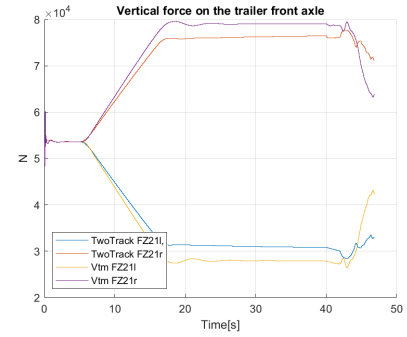

(h) Vertical load on trailer front axle.

Figure 2.11: Simulation results of the single-track model, two-track model, and VTM in cornering and strong braking test at 40 km/h and $\mu = 0.3$ with conservativity $e = 1.1$

In contrast with the Pacejka tire model, friction circle-inspired combined slip model is more conservative for small longitudinal slips, i.e., the reduction in lateral force is greater than the Pacejka tire model when longitudinal slips are small. Consequently, the two-track model captures jackknife under more gentle driving conditions, such as situations with less braking force and reduced steering angle, whereas the VTM may not capture jackknife events.

By incorporating an increased conservativity $e = 1.1$ in the tire model, the two-track model exhibits improved alignment with the dynamics described by the VTM in instances involving both the gentle braking and strong braking cases. For the gentle braking case, as shown in Figure 2.8 with an increased convervativity $e = 1.1$, the two-track model suggests the truck is safe, which is assigned with the outcomes from the VTM. In the strong braking case, as shown in Figure 2.11 the two-track model with $e = 1.1$ exhibits a jackknifing time closer to that observed in the VTM compared to the case with $e = 1$. These findings provide compelling evidence for attributing the substantial disparities to the conservativity factor of the tire model.

3

Design of Jackknifing Prevention Safety System

This chapter outlines the procedure for designing and implementing the prediction algorithm. Initially, the obtained time-continuous single-track and two-track models are discretized using the Euler method. Subsequently, the discussion encompasses the assumptions and methodology employed to predict the driver's future behavior. Lastly, this chapter presents the algorithms and steps involved in predicting the future states of the vehicle.

3.1 System Discretization for Single-track Model

Motion models derived from Chapter 2 are continuous-time models. Continuous-time systems need to be discretized because measurements in reality are sampled. Euler method is a good technique to approximate differential equations that makes use of linear approximation [19]:

$$x(t + T_s) \approx x(t) + T_s \cdot f(x(t), u(t)) \tag{3.1}$$

Using the Euler method the discretized single-track model becomes:

$$\underbrace{\begin{bmatrix} x_1[n+1] \\ x_2[n+1] \\ x_3[n+1] \\ x_4[n+1] \\ x_5[n+1] \end{bmatrix}}_{\boldsymbol{x[n+1]}} = \underbrace{\begin{bmatrix} x_1[n] \\ x_2[n] \\ x_3[n] \\ x_4[n] \\ x_5[n] \end{bmatrix}}_{\boldsymbol{x[n]}} + T_s \underbrace{\begin{bmatrix} f_1(x[n], u[n]) \\ f_2(x[n], u[n]) \\ f_3(x[n], u[n]) \\ x_5[n] \\ f_4(x[n], u[n]) \end{bmatrix}}_{\boldsymbol{f(x[n],u[n])}} \tag{3.2}$$

where $T_s = 0.01$ represents the time step value used for discretization.

3.2 System Discretization for Two-track Model

Incorporating the dynamics of vertical forces introduces a challenge during the construction of the state space system. The challenge arises from the fact that the acceleration of the CoG affects the tire loads, which, in turn, affects the lateral forces from tires. Conversely, the lateral force is required to determine the acceleration of the CoG. The interdependence problem can be addressed by introducing a first-order lag model [20]. This model assumes that the accelerations of CoG do not

reach their steady value immediately.

The states for the two-track model augmented by the accelerations are:

$$x = \begin{bmatrix} v_{x_1} & v_{y_1} & \dot{\phi}_1 & \theta & \dot{\theta} & a_{y1p} & a_{y2p} & a_{x1p} \end{bmatrix}^T \tag{3.3}$$

where the derivative of GoG's acceleration is given by the first-order filter:

$$\dot{a}_{y1p} = \frac{1}{\tau_{Lat}}(a_{y1} - a_{y1p}) = \frac{1}{\tau_{Lat}}(\dot{v}_{y1} + \dot{\phi} v_{x1} - a_{y1p}) \tag{3.4}$$

$$\dot{a}_{y2p} = \frac{1}{\tau_{Lat}}(a_{y1} - a_{y1p}) = \frac{1}{\tau_{Lat}}(\dot{v}_{y2} + \dot{\phi} v_{x2} - a_{y2p}) \tag{3.5}$$

$$\dot{a}_{x1p} = \frac{1}{\tau_{Lat}}(a_{y1} - a_{y1p}) = \frac{1}{\tau_{Lat}}(\dot{v}_{x1} - \dot{\phi} v_{y1} - a_{x1p}) \tag{3.6}$$

where τ_{Lat} is chosen as 0.05. The derivative of v_{x1}, v_{y1},v_{y2} can be obtained by using the model equations presented earlier. The two-track model is discretized using the Euler method.

3.3 Driver behavior prediction

The predictor uses the discrete single-track/two-track state space model to predict the future behavior of the vehicle. At time step n, the initial value $x[n|n]$ is determined using measurements. Subsequently, at the prediction step 1, the discrete state transition model $f(\hat{x}[n+1|n], \hat{u}[n+1|n])$ is applied to predict the next state vector $\hat{x}[n+2|n]$ given the current predicted state vector $\hat{x}[n+1|n]$ and predicted input $\hat{u}[n+1|n]$. By repeating the predict step for a total of M times, with a system sampling time of T_s, the predictor foresees the behavior of the vehicle over $T_s \cdot M$ seconds.

$$\hat{x}[n+1+M|n] = x[n|n] + T_s \sum_{m=0}^{M-1} f(\hat{x}[n+m|n], \hat{u}[n+m|n]) \tag{3.7}$$

Despite having a discrete single-track/two-track state space model, the predictor still needs the future driver behavior as input to predict the truck's motion, $u[n+m|n]$. In this section, we will introduce some ways to facilitate the driver input to the predictor. A block diagram in Figure 3.1 shows different ways of feeding driver information to the predictor.

The driver information consists of two parts, steering actions and pedal actions. The prediction model relies on constant input signals. For the steering, the predictor assumes a constant steering angle, $\hat{\delta}[n+m|n] = \delta[n],\ m = 1, 2 \ldots M$, where M is the prediction horizon. For the pedal action, when the driver presses the pedal to brake, the brake force applied to the wheels may not align with the driver's requested brake force, due to several reasons. Firstly, the requested brake forces are adjusted by the slip controller to avoid excessive longitudinal slip, as illustrated in Figure 3.1. Subsequently, these adjusted brake forces, coming from the slip controller, are sent

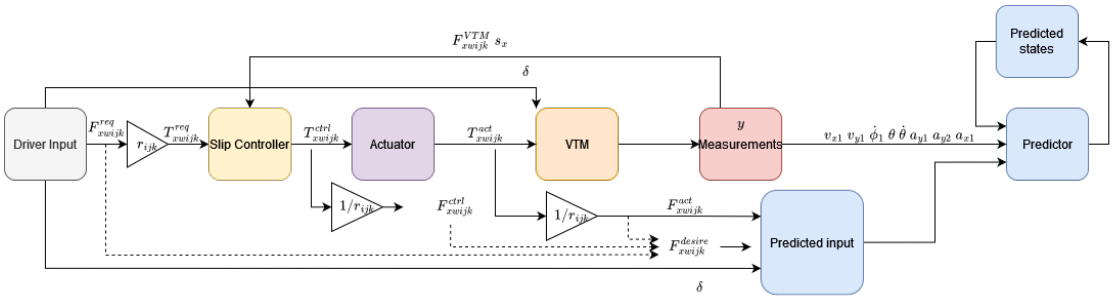

Figure 3.1: Block diagram illustrating the different ways to feed driver information to the predictor.

to the actuator, which requires some time to respond. As a consequence of this, different approaches for feeding constant driver input signals are used.

The first approach uses constant pedal action directly from the driver's braking pedal, $\hat{F}^{req}_{xwijk}[n+m|n] = F^{req}_{xwijk}[n],\ m = 1, 2 \dots M$ is constant over the prediction horizon M. The second approach uses the signals from the slip controller, $\hat{F}^{ctrl}_{xwijk}[n+m|n] = F^{ctrl}_{xwijk}[n],\ m = 1, 2 \dots M$. As an electric motor is used as an actuator, the system model needs to be augmented with an actuator model. The actuator model is, as mentioned earlier, represented as a first-order system:

$$F_{xw,act} = G_{act}(s)F_{xw,des} = \frac{1}{\tau_{act} \cdot s + 1} F_{xw,des} \tag{3.8}$$

where τ_{act} is the actuator time constant, and $F_{xw,des}$ is either F^{req}_{xwijk} or F^{ctrl}_{xwijk} depending on approach. The first-order continuous time transfer function of $G_{act}(s)$ is discretized using forward Euler discretization method by replacing s with $\frac{z-1}{T}$, resulting in

$$G_{act}(z) = \frac{1}{\frac{\tau_{act} \cdot z - \tau_{act}}{T_s} + 1} \tag{3.9}$$

where T_s is the sampling time. The resulting discrete-time model can now be written as:

$$F_{xw,act}[n+1] = c_1 F_{xw,act}[n] + c_2 F_{xw,des}[n] \tag{3.10}$$

where c_1 and c_2 depend on the actuator time constant and sampling time. With a sampling time of $T_s = 0.01$ s, and an actuator time constant of $\tau_{act} = 0.2$, c_1 becomes 0.95 and c_2 becomes 0.05. With a time constant of $\tau_{act} = 1$ s, c_1 becomes 0.99 and c_2 becomes 0.01.

The last approach is to use the signal from the actuator to the predictor, $\hat{F}^{act}_{xwijk}[n+m|n] = F^{act}_{xwijk}[n],\ m = 1, 2 \dots M$. In this case, the system model does not need to be augmented with the actuator model.

One limitation of using longitudinal forces as input and employing the ellipse combined slip model is that input wheel forces, represented by F_{xwijk} must fall within the range of $-\mu \cdot F_{Zwijk}$ to $\mu \cdot F_{Zwijk}$. As a result, the predicted longitudinal forces

must be corrected to ensure they do not exceed the range before updating the current state for each time step. In the single-track model, where the vertical load on each wheel is constant, we can easily assign the value $\pm\mu F_{zij}$ to the predicted longitudinal force $\hat{F}_{xwpredij}[n+m|n]$, if it exceeds the friction limit $\pm\mu F_{zij}$.

Furthermore, the situation becomes more complex in the two-track model, where the vertical load varies after each time step because the states a_{x1p}, a_{y1p}, and a_{y2p} determines the vertical load. Hence, it is essential to calculate the vertical load on each wheel to determine the range of the brake force before sending the longitudinal force to the discrete state space model.

$$F_{xwijk} < \mu \cdot f_{zijk} \tag{3.11}$$

where f_{zijk} represents the nonlinear equations used to compute the vertical loads on the wheels.

The prediction model is implemented in MATLAB in symbolic expressions. To improve prediction computing speed, `matlabFunction` [21] is used to covert symbolic equations to function handle, expressed as `f_func`. Sampling time is set when generating the function handle. The road friction coefficient μ and conservativity of tire model e are variables to be set, which means that for different road friction conditions and conservativity, `f_func` has to be updated. Algorithm 1 and Algorithm 2 show the predictors' state prediction steps.

Algorithm 1 State prediction for single-track predictor

for n `in simulation time` **do**
  $\hat{u}[n|n] = [F_{xw11}\ F_{xw12}\ F_{xw21}\ F_{xw22}\ \delta]$ ▷ Inputs at time step `n`
  $\hat{x}[n|n] = [v_{x_1}\ v_{y_1}\ \dot{\phi}_1\ \theta\ \dot{\theta}]$
  for `m in` M **do**
    if $|F_{xwijk}| \notin [0, \mu F_{zijk}]$ **then**
      $F_{xwijk} = \pm\mu F_{zijk}$
    end if
    $\hat{x}[n+m+1|n] =$ `f_func`$(\hat{x}[n+m|n], \hat{u}[n+m|n])$ ▷ Model update
  end for
end for

3.4 Jackknifing Detection and Prediction Method

Currently, there has been limited discussion in the literature regarding indicators or detectors for jackknifing [3]. The most straightforward trait of jackknifing is that the articulation angle will reach a significant value. However, using an indicator based on articulation angle is not sufficient to provide the detection at an early stage. Since jackknifing is a severe yaw instability, the yaw rate of tractor $\dot{\phi}_1$ is strongly

Algorithm 2 State prediction for two-track predictor

for n `in simulation time` **do**
$\hat{u}[n|n] = [F_{xw11l}\ F_{xw12l}\ F_{xw21l}\ F_{xw22l}\ F_{xw11r}\ F_{xw12r}\ F_{xw21r}\ F_{xw22r}\ \delta_n]$ ▷ Inputs at time step `n`
$\hat{x}[n|n] = [v_{x1_n}\ v_{y1_n}\ \dot{\phi}_{1_n}\ \theta_n\ \dot{\theta}_n\ a_{y1p_n}\ a_{y2p_n}\ a_{x1p_n}]$
$u_{desire}[n] = [F_{xw11ld}\ F_{xw11rd,n}\ F_{xw12ld}\ F_{xw12rd}\ F_{xw21ld}\ F_{xw21rd}\ F_{xw22ld}\ F_{xw22rd}\ \delta_n]$ ▷ Desired input at time step `n`
for `m in` $Horizon$ **do** ▷ Predict $Horizon$ time steps
$\hat{u}[n+m+1|n] = c_1\hat{u}[n+m|n] + c_2 u_{desire}[n]$ ▷ $c_1 = 0.95$ and $c_2 = 0.05$ for $\tau_{pred} = 0.2$, $c_1 = 0.99$ and $c_2 = 0.01$ for $\tau_{pred} = 1$. $F_{xwpred11l}$, $F_{xwpred11r}$, δ_{pred} keeps constant with $F_{xw11l,n}$, $F_{xw11r,n}$, δ_n
end for
for `M in` $Horizon$ **do**
if $|\hat{u}[n+m|n](2)| \notin [0, \mu f_{z12l}(\hat{x}[n+m|n], \hat{u}[n+m|n])$ **then**
$\hat{u}[n+m|n](2) = \pm\ \mu f_{z12l}(x[n+m|n], u[n+m|n])$ ▷ instead of using $\mu = 0.3$, here $\mu = 0.29$ to avoid exceeding friction limit
end if
if $|\hat{u}[n+m|n](6)| \notin [0, \mu f_{z12r}(\hat{x}[n+m|n], \hat{u}[n+m|n])]$ **then**
$\hat{u}[n+m|n](6) = \pm\ \mu f_{z12r}(\hat{x}[n+m|n], \hat{u}[n+m|n])$
end if
$\hat{x}[n+m+1|n] =$ `f_func`$(\hat{x}[n+m|n], \hat{u}[n+m|n])$ ▷ Update discrete process model one time step
end for
end for

related. The reference yaw rate, which serves as the desired yaw rate when a truck is safely cornering, is calculated using a linear vehicle model:

$$\dot{\phi}_{ref} = \frac{v_{x_1} \cdot \delta}{L_1} \tag{3.12}$$

$$|\dot{\phi}_1 - \dot{\phi}_{ref}| \leq 0.1 \tag{3.13}$$

The predicted yaw rate reference in Equation 3.12 is determined by the future predicted longitudinal speed of the tractor and predicted input steering angle, where L_1 is the wheelbase of the tractor.

The employed prediction method involves comparing the magnitude of the deviation between the tractor's future yaw rate and the predicted yaw rate reference to a threshold, as expressed in Equation 3.13. The threshold value of the yaw rate difference is set to 0.1. When safely driving the vehicle, if the absolute value of Equation 3.13 is less than or equal to 0.1, it indicates that the current driver maneuver is considered safe and jackknife is less likely to occur in the future. Conversely, if the absolute value exceeds 0.1, it suggests that the truck tends to jackknife in the future.

The threshold value is a trade-off between early detection and detection triggering. A too-low threshold may lead to numerous false detections, even when the driver's maneuver is safe. On the other hand, if the threshold is set too high, there is a risk of detecting the jackknife situation too late, and the action taken to prevent the jackknife may also occur too late to avoid it. Thus, the chosen value aims to keep a balance between accurate prediction and timely response to avoid jackknifing.

4

Results and Discussions

This chapter begins with creating test cases by setting up different simulation conditions. Secondly, the validation results of single- and two-track predictors in predicting and preventing jackknifing are presented. Then, from the simulation results, the boundaries of the two predictors' effectiveness are explored, and comparisons of the two predictors are made. Finally, factors that influence the effectiveness of the predictor are analyzed.

4.1 Test Cases

There are nine sets of test cases conducted, which includes three different initial longitudinal speed v_{x0}, and three brake types are tested separately at each of the initial longitudinal speed scenarios. The proposed predictor was employed on VTM's tractor-semi-trailer combination in all test cases.

4.1.1 Road Condition

The tests were conducted with a predetermined turning radius of 72m on the snowy ground, with a coefficient of friction of $\mu = 0.3$. Throughout the simulations, tire rolling resistance is negligible.

4.1.2 Driver Maneuver Description

The initial steering is zero, followed by a ramp signal that starts after 5 seconds. The ramp signal has a fixed slope of 5×10^{-3}, which is stopped at the maximum steering angle limit δ_{lim}. The initial longitudinal speeds are $v_{x0} = [35,\ 40,\ 43]$ km/h for various trails. To maintain the fixed turning radius of 72m, the respective steering angles' upper limit for these initial velocities are $\delta_{lim} = [0.05198,\ 0.0542,\ 0.06032]$ rad.

During cornering and braking, the steering angle remains constant. The brake types are categorized as gentle, moderate, and strong braking, with the corresponding requested total braking force F_{brake}^{req} set to -10000, -20000, and -30000 N, respectively.

The trajectory begins with a straight path, transitioning into a curve that connects the straight and circular tracks as the steering angle increases. When the steering angle reaches its upper limit, the truck is in a circular motion with a radius of 72m.

The braking action is initiated at 40^{th} second, by which time the truck is already on the circular route, with the requested braking force acting on the tractor's rear wheels. In all scenarios, the truck corners left while braking.

4.1.3 Predictor Setup

As discussed earlier, the longitudinal forces prediction involves the utilization of two inputs: the current longitudinal forces on each wheel from the actuator and the driver desired forces F_{xwdes} for each wheel. The driver's desired braking forces can originate from three distinct sources: the braking forces requested by the driver upon pressing the pedal, the braking forces specified by the longitudinal slip controller, and the braking forces generated by the actuator. To simplify nomenclature, we call them request braking force F_{xw}^{req}, controller braking force F_{xw}^{ctrl} and actuator braking force F_{xw}^{act}. The trails include the results of using all three types of desired braking forces.

Two values, $\tau_{act} = [0.2,\ 1]$, are assigned to the time constants of the first-order filter used for predicting future driver input. Predicted horizon were varied, with values of [0.1, 1, 2, 3]s being considered. Simulation termination conditions included the longitudinal speed dropping below 2 m/s or the truck's articulation angle reaching 60°.

4.1.4 Performance Metric

Based on the aforementioned scenarios, 216 simulations were executed for both the single-track and two-track predictors, respectively. All results are presented in Appendix B. The performance metric includes three distinct time values and two categories of time difference, t_0 the reference time when the yaw rate difference of the VTM reaches the threshold 0.1, t_1 is the first-time point at which the predicted yaw rate difference attains the predefined threshold, and t_2 indicates the closest time when the predicted yaw rate difference reaches the threshold to the time t_0. The predictor could issue warnings even when the VTM does not experience jackknifing for a considerable duration. This phenomenon could lead to frequent warnings being triggered without the actual occurrence of jackknifing.

In addition, the corresponding time differences, Δt_1 and Δt_2, which indicates the differences between t_1 and t_2 to t_0 is also used as a performance metric:

$$\begin{aligned} \Delta t_1 &= t_1 - t_0 \\ \Delta t_2 &= t_2 - t_0 \end{aligned} \tag{4.1}$$

The positive value of Δt_1 indicates the predictor foresees the occurrence of jackknifing. Conversely, the negative value of Δt_1 indicates the predictor fails to predict jackknifing. The mismatch between Δt_1 and Δt_2 suggests that there exists a period during the predictor foresees the truck's future motion is safe after the initial warning, the predictor makes an overly aggressive assumption about the driver future input.

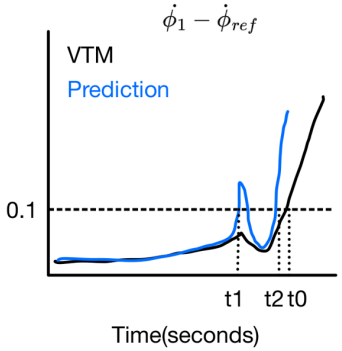

Figure 4.1: Illustration of t_1, t_2 and t_0. The black line is the yaw rate reference from the VTM ground truth and the blue line is the predicted yaw rate reference with n seconds time horizon given current states measurement

4.2 Single-Track Predictor

The comprehensive set of results for the single-track predictor is incorporated within the Appendix B.1. Subsequent sections provide illustrative instances to showcase the outcomes derived from the single-track predictor.

4.2.1 Illustration of Motion Prediction for A Non-jackknife Case

Figure 4.2 illustrates various predicted states for a test scenario with an initial longitudinal speed of 40 km/h and a requested braking force of -10000 N. The predictor is configured using the single-track model, $\tau_{act} = 0.2$, and $F_{xwdes} = F_{xw}^{act}$, in situation where the jackknifing does not occur. The figure illustrates the predicted states $\hat{x}$ for the different time horizons.

The predicted state values align well with the value given by the VTM in general. Specifically, when the truck is braking and after 43^{th} second, the values of predicted states generated by the predictor with different time horizons nearly match the values given by the VTM.

During the time 20^{th} second to 40^{th} second when the truck is steady cornering, there exists a noticeable error from the different predicted states as shown in Figure 4.5b, Figure 4.5c and Figure 4.5d, to the VTM value when the predicted time horizon is [1, 2, 3]. Because the driver input remains unchanged during this period, the predicted driver input perfectly matches the future scenario. These discrepancies suggest the inaccuracy of the dynamics model within the predictor. Consequently, during this time interval, albeit the predicted driver input perfectly matches the future driver input, the measured states deviate and evolve from their expected steady values to new steady values determined by the inaccurate dynamic model.

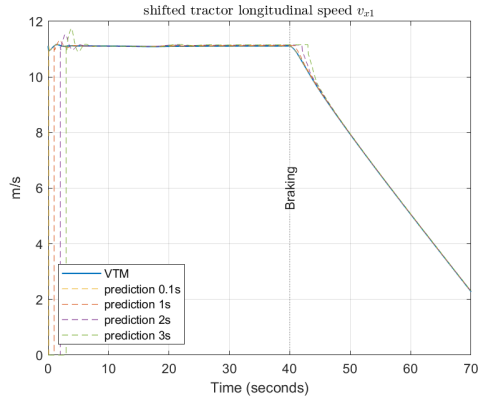

(a) Tractor longitudinal speed v_{x1}

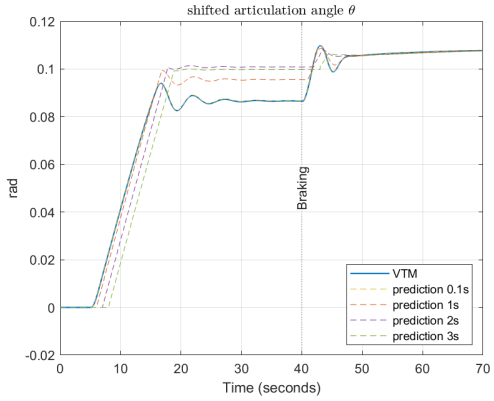

(b) Articulation angle θ

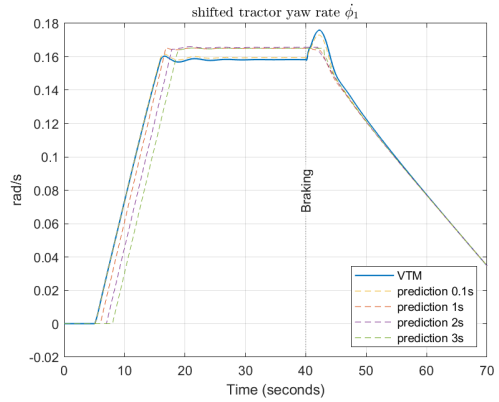

(c) Tractor yaw rate $\dot{\phi}_1$

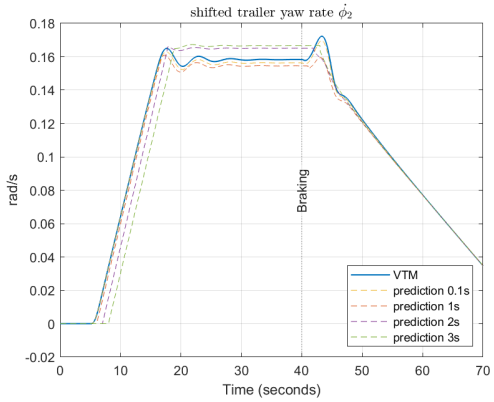

(d) Trailer yaw rate $\dot{\phi}_2$

Figure 4.2: Non-jackknife case - state prediction results of single-track predictor with sample time = 0.01s, $v_{x0} = 40$km/h, $F^{req}_{brake} = -10000$ N, $\tau_{pred} = 0.2$, $F_{xwdesire} = F^{act}_{xw}$

Between the time interval 5^{th} second to 15^{th} second, the predicted states generated by different time horizon predictors do not match well with each other. The discrepancy arises due to the varying propelling forces of the truck during this stage, and the magnitude of future input forces is different for different time horizon predictors. For instance, at time 10^{th} second, the predicted states provided by the predictor with $3s$ time horizon rely on the wheel forces at 7^{th} second to predict driver future input. On the other hand, the predicted states provided by the predictor with $1s$ time horizon rely on the wheel forces at 9^{th} second.

4.2.2 Illustration of Motion Prediction for A Jackknife Scenario

Table 4.1 presents the results for a scenario with an initial longitudinal speed of 40 km/h, a request braking force of -30000 N, using a predictor time of $\tau_{pred} = 0.2$. Within this scenario, a comparison among predictors with different desired brake force sources from F^{req}_{xw}, F^{ctrl}_{xw}, F^{act}_{xw} is presented in Figure 4.3 in terms of yaw rate difference. In addition, the predicted results of tractor yaw rate $\dot{\phi}_1$ are also shown

in Figure 4.4.

Table 4.1: Performance table (Single-track, Sample time = 0.01s, v_{x0} = 40 km/h, $F_{brake}^{req} = -30000$ N, $\tau_{pred} = 0.2$)

Desired Force	Predicted Time Length	VTM t_0 (s)	Predicted t_1 (s)	Predicted t_2 (s)	Δt_1 (s)	Δt_2 (s)	Action prevent jackknife
F_{xw}^{req}	0.1s	46.24	46.29	46.29	+0.05	+0.05	Success
F_{xw}^{req}	1s	46.24	40.02	40.02	-6.22	-6.22	Success
F_{xw}^{req}	2s	46.24	40.02	40.02	-6.22	-6.22	Success
F_{xw}^{req}	3s	46.24	40.02	40.02	-6.22	-6.22	Success
F_{xw}^{ctrl}	0.1s	46.24	46.32	46.32	+0.08	+0.08	Fail
F_{xw}^{ctrl}	1s	46.24	40.01	46.47	-6.23	+0.23	Success
F_{xw}^{ctrl}	2s	46.24	40.01	46.50	-6.23	+0.26	Success
F_{xw}^{ctrl}	3s	46.24	40.01	46.51	-6.23	+0.27	Success
F_{xw}^{act}	0.1s	46.24	46.32	46.32	+0.08	+0.08	Fail
F_{xw}^{act}	1s	46.24	46.45	46.45	+0.23	+0.23	Fail
F_{xw}^{act}	2s	46.24	46.48	46.48	+0.24	+0.24	Fail
F_{xw}^{act}	3s	46.24	46.50	46.50	+0.26	+0.26	Fail

4.3 Two-Track Predictor

The two-track predictor was also tested by the same scenarios as the single-track predictor, and the outcomes are detailed in Appendix B.2. The sole difference lies in the brake force input. In cases of the single-track predictor, the input longitudinal forces for the same axle are the sum of the forces acting on the left and right wheels. However, in the case of the two-track predictor, the input longitudinal forces acting on the left and right wheels of the same axle are treated as separate entities.

4.3.1 Simulation Results

4.3.1.1 Non-jackknife Cases

Figure 4.5 presents the predicted states' results of a non-jackknife case, following the identical scenario in Section 4.2.1.

4.3.1.2 Jackknife Cases

The prediction result of the same scenarios is presented in Table 4.2. Figure 4.6 shows the yaw rate difference, and Figure 4.7 shows the desired brake force comparison and the tractor yaw rate. From the performance table, it can be seen that the two-track model can successfully predict and prevent jackknifing in these 12

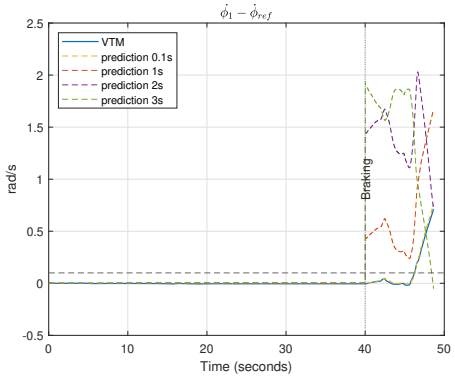

(a) $F_{xwdesire} = F_{xw}^{req}$ as input

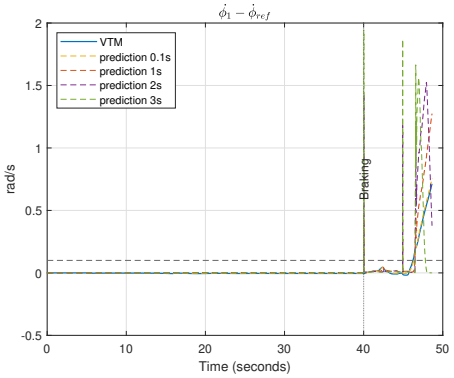

(b) $F_{xwdesire} = F_{xw}^{ctrl}$ as input

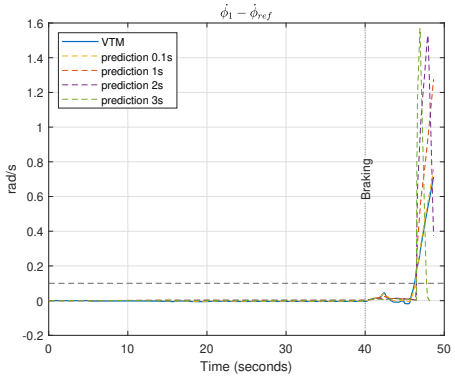

(c) $F_{xwdesire} = F_{xw}^{act}$ as input

Figure 4.3: Jackknife case - yaw rate difference $\dot{\phi}_1 - \dot{\phi}_{ref}$ of different $F_{xwdesire}$ of the single-track predictor with sample time = 0.01s, $v_{x0} = 40$ km/h, $F_{brake}^{req} = -30000$N, $\tau_{pred} = 0.2$

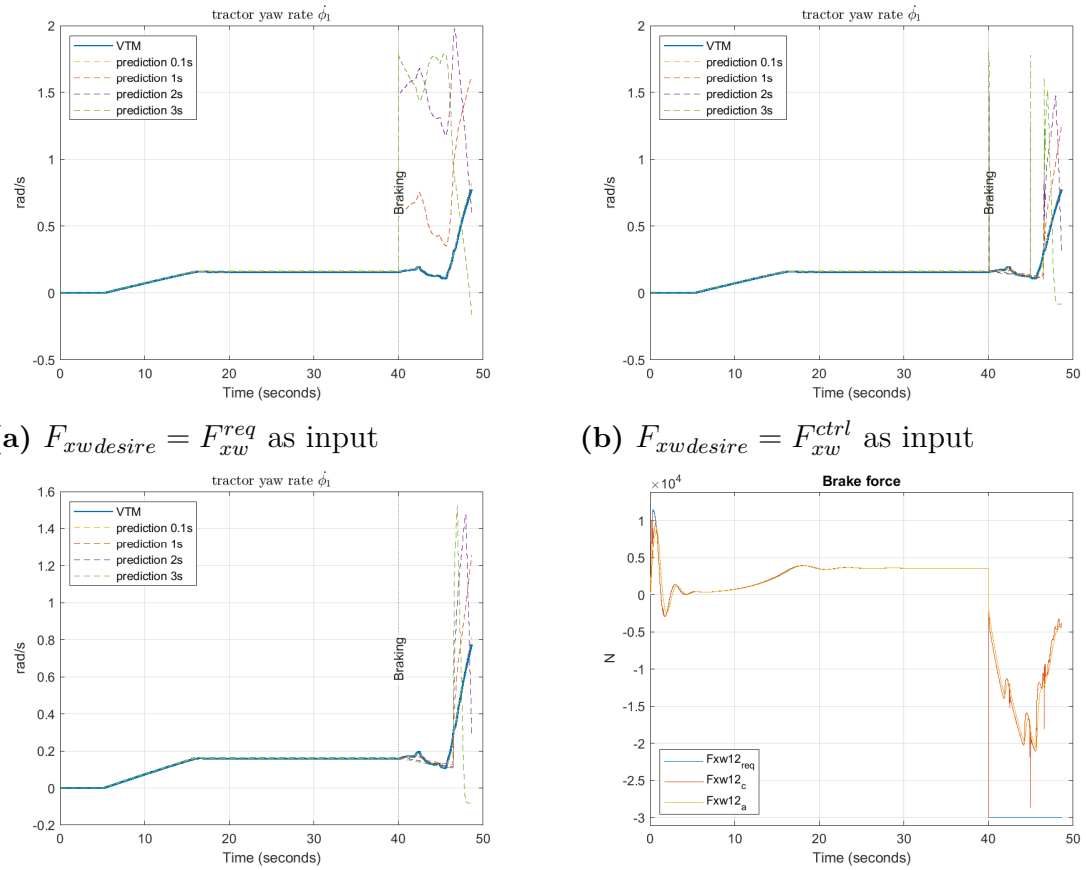

(a) $F_{xwdesire} = F_{xw}^{req}$ as input

(b) $F_{xwdesire} = F_{xw}^{ctrl}$ as input

(c) $F_{xwdesire} = F_{xw}^{act}$ as input

(d) F_{xw}^{req}, F_{xw}^{ctrl}, F_{xw}^{act} comparison

Figure 4.4: Jackknife case - tractor yaw rate $\dot{\phi}_1$ of different $F_{xwdesire}$ and brake force comparison of the single-track predictor with sample time = 0.01s, $v_{x0} = 40$km/h, $F_{brake}^{req} = -30000$ N, $\tau_{pred} = 0.2$

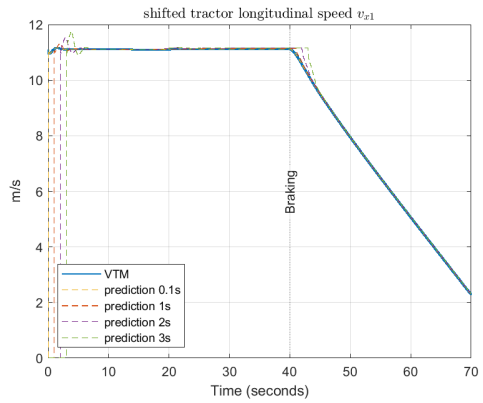

(a) Tractor longitudinal speed v_{x1}

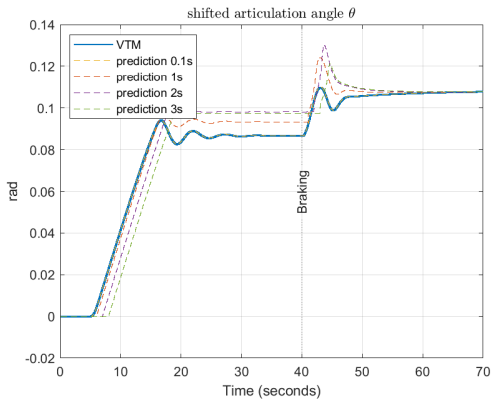

(b) Articulation angle θ

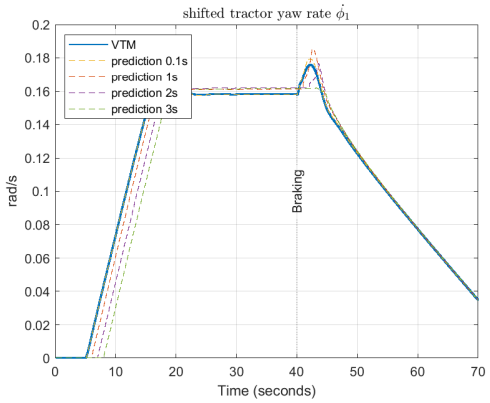

(c) Tractor yaw rate $\dot{\phi}_1$

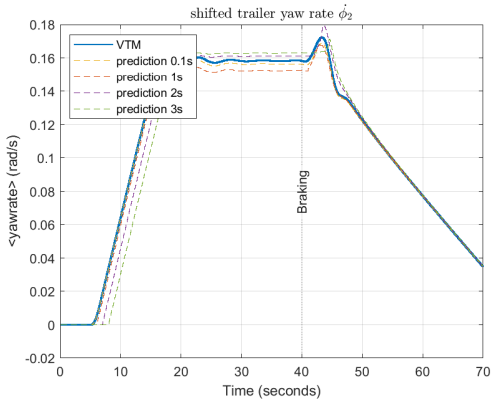

(d) Trailer yaw rate $\dot{\phi}_2$

Figure 4.5: Non-jackknife case - state prediction results of the two-track predictor with sample time = 0.01s, $v_{x0} = 40$ km/h, $F_{brake}^{req} = -10000$ N, $\tau_{pred} = 0.2$, $F_{xwdesire} = F_{xw}^{act}$

cases, which illustrates that the two-track predictor is better than the single-track predictor.

Table 4.2: Performance table (Two-track, Sample time = 0.01s, v_{x0} = 40km/h, $F_{brake}^{req} = -30000$ N, $\tau_{pred} = 0.2$)

Desired Force	Predicted Time Length	VTM t_0 (s)	Predicted t_1 (s)	Predicted t_2 (s)	Δt_1 (s)	Δt_2 (s)	Action prevent jackknife
F_{xw}^{req}	0.1s	46.24	46.22	46.22	-0.02	-0.02	Success
F_{xw}^{req}	1s	46.24	40.24	45.94	-6.00	-0.30	Success
F_{xw}^{req}	2s	46.24	40.01	40.01	-6.23	-6.23	Success
F_{xw}^{req}	3s	46.24	40.01	40.01	-6.23	-6.23	Success
F_{xw}^{ctrl}	0.1s	46.24	46.25	46.25	+0.01	+0.01	Success
F_{xw}^{ctrl}	1s	46.24	41.73	46.20	-4.51	-0.04	Success
F_{xw}^{ctrl}	2s	46.24	40.01	46.20	-6.23	-0.04	Success
F_{xw}^{ctrl}	3s	46.24	40.01	46.19	-6.23	-0.05	Success
F_{xw}^{act}	0.1s	46.24	46.25	46.25	+0.01	+0.01	Success
F_{xw}^{act}	1s	46.24	46.23	46.23	-0.01	-0.01	Success
F_{xw}^{act}	2s	46.24	41.58	46.23	-4.66	-0.01	Success
F_{xw}^{act}	3s	46.24	41.51	46.23	-4.73	-0.01	Success

Table 4.3 presents simulation results of initial longitudinal speed 43 km/h, request braking force -10000 N, $\tau_{pred} = 0.2$. Even if the brake is gentle, the vehicle will still jackknife at this initial speed.

4.4 Single-track and Two-track Predictor Comparison

Figure 4.8 is the histograms that provide a visual representation of the distribution for the predicted Δt_1 values when given by the single-track model and two-track model across 120 testing cases where jackknifing occurs. These tests involve varying predictor setup, initial velocities and F_{brake}^{req}.

It is assumed that if the Δt_1 value is negative, the predictor anticipates jackknifing in advance (true positive). If the Δt_1 value is positive or zero, the predictor does not anticipate jackknifing in advance, leading to incorrectly predicted non-jackknifing events (false negative). When the predictor incorrectly predicted jackknifing events while the vehicle was safe, it is considered a false positive. And if the predictor does not give a jackknifing warning and the vehicle does not jackknife, it is labeled as a true negative. Figure 4.9 shows the confusion matrices of 216 tests for both the

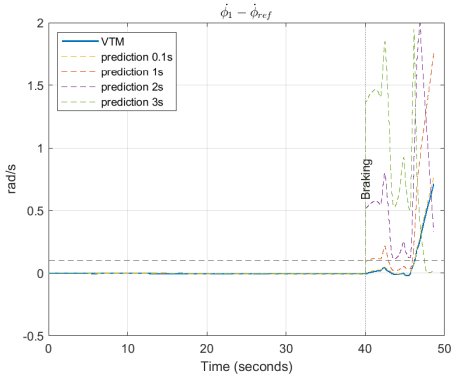

(a) $F_{xwdesire} = F_{xw}^{req}$ as input

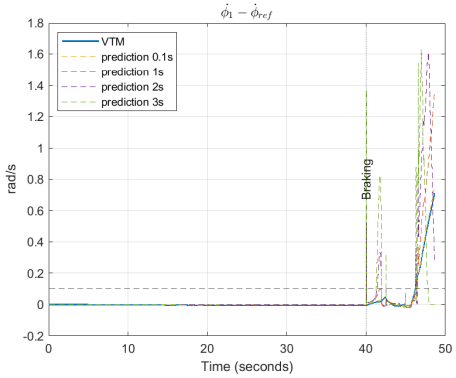

(b) $F_{xwdesire} = F_{xw}^{ctrl}$ as input

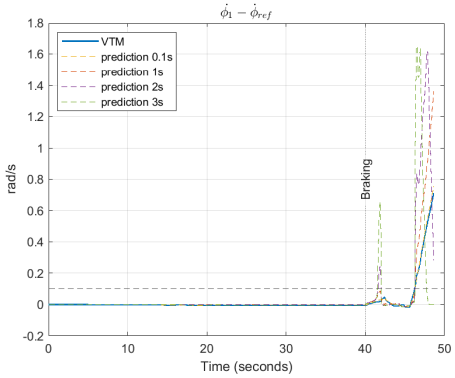

(c) $F_{xwdesire} = F_{xw}^{act}$ as input

Figure 4.6: Jackknife case - yaw rate difference $\dot{\phi}_1 - \dot{\phi}_{ref}$ of different $F_{xwdesire}$ of the two-track predictor with sample time = 0.01s, $v_{x0} = 40$ km/h, $F_{brake}^{req} = -30000$N, $\tau_{pred} = 0.2$

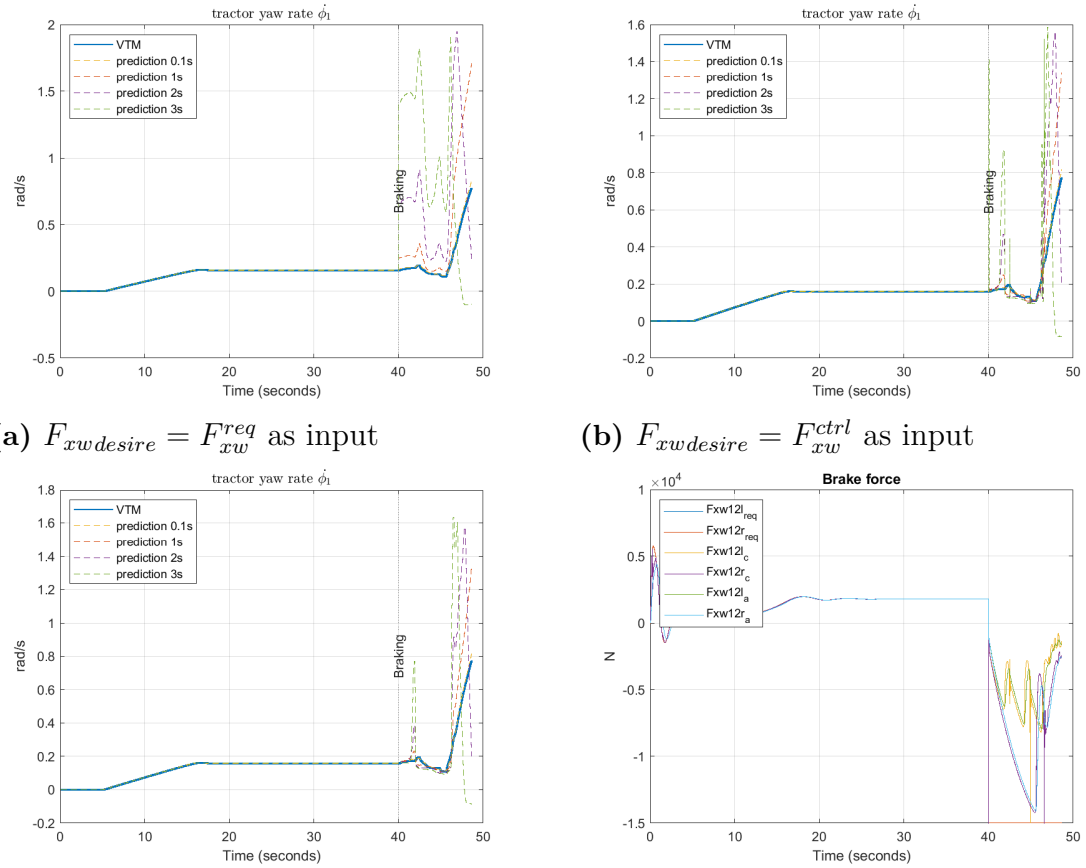

(a) $F_{xwdesire} = F_{xw}^{req}$ as input

(b) $F_{xwdesire} = F_{xw}^{ctrl}$ as input

(c) $F_{xwdesire} = F_{xw}^{act}$ as input

(d) F_{xw}^{req}, F_{xw}^{ctrl}, F_{xw}^{act} comparison

Figure 4.7: Jackknife case - tractor yaw rate $\dot{\phi}_1$ of different F_{xw}^{desire} and brake force comparison of two-track predictor with sample time = 0.01s, $v_{x0} = 40$ km/h, $F_{brake}^{req} = -30000$ N, $\tau_{pred} = 0.2$

Table 4.3: Prediction results (Two-track, Sample time = 0.01s, v_{x0} = 43 km/h, $F_{brake}^{req} = -10000$ N, $\tau_{pred} = 0.2$)

Desired Force	Predicted Time Length	VTM t_0 (s)	Predicted t_1 (s)	Predicted t_2 (s)	Δt_1 (s)	Δt_2 (s)	Action prevent jackknife
F_{xw}^{req}	0.1s	42.55	42.41	42.41	-0.14	-0.14	Fail
F_{xw}^{req}	1s	42.55	40.34	40.34	-2.21	-2.21	Success
F_{xw}^{req}	2s	42.55	40.01	40.01	-2.54	-2.54	Success
F_{xw}^{req}	3s	42.55	40.01	40.01	-2.54	-2.54	Success
F_{xw}^{ctrl}	0.1s	42.55	42.45	42.45	-0.1	-0.1	Fail
F_{xw}^{ctrl}	1s	42.55	41.03	41.03	-1.52	-1.52	Success
F_{xw}^{ctrl}	2s	42.55	40.01	40.67	-2.54	-1.88	Success
F_{xw}^{ctrl}	3s	42.55	40.01	40.51	-2.54	-2.04	Success
F_{xw}^{act}	0.1s	42.55	42.43	42.43	-0.12	-0.12	Fail
F_{xw}^{act}	1s	42.55	41.14	41.14	-1.41	-1.41	Success
F_{xw}^{act}	2s	42.55	40.84	40.84	-1.71	-1.71	Success
F_{xw}^{act}	3s	42.55	40.71	40.71	-1.84	-1.84	Success

single-track and two-track model.

These results from the two-track predictor do not exhibit a stronger advantage over the outcomes from the single-track predictor. Although the two-track predictor shows a higher count of true positive cases than the single-track predictor, it also experiences an increase in false positive predictions.

One potential explanation can be the limited scope of testing carried out. The predictor setup is not standardized, with parameters like varying prediction horizon lengths, diverse sources of the desired forces, and distinct predictor time constant τ_{pred} contributing to the overall conservativeness of the predictor. The various predictor setups can improve the capability of the single-track predictor in anticipating jackknifing. Furthermore, the selection of testing cases includes many scenarios with an initial speed of 43 km/h, representing an extremely challenging condition. In these extreme cases, it becomes relatively easier for the single-track model to predict the occurrence of jackknifing.

The single-track model employs a simplified approach by lumping multiple wheels on the same axle into a single virtual wheel. This model determines the lateral forces by summing up the longitudinal forces of the left and right wheels. However, this approach proves inadequate as it forecasts jackknifing when the virtual wheels yield insufficient lateral forces, which does not align with complex real-world dynamics. Due to the load transfer, the friction limit for the wheel on the same axle varies, which is ignored by the single-track model. The inner wheel is prone to losing grip

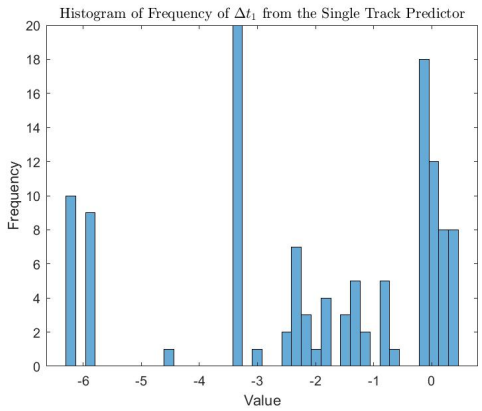

(a) Δt_1 from the single track predictor

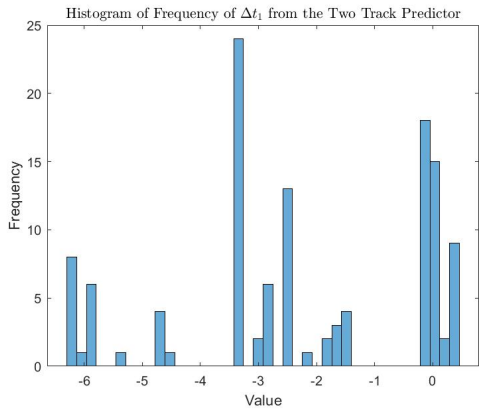

(b) Δt_1 from the two-track predictor

Figure 4.8: Histogram of Δt_1 for cases when jackknifing occurs under varying predictor setup, initial velocity and F_{brake}^{req}.

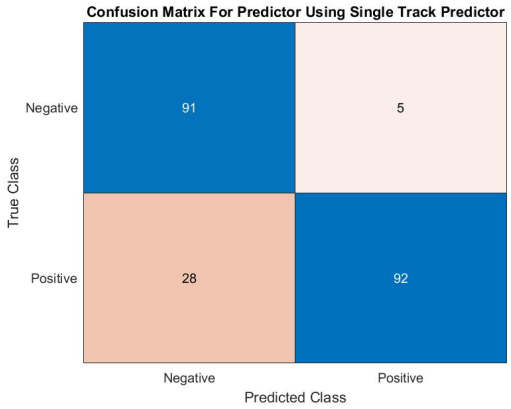

(a) Confusion matrix of the single track predictor

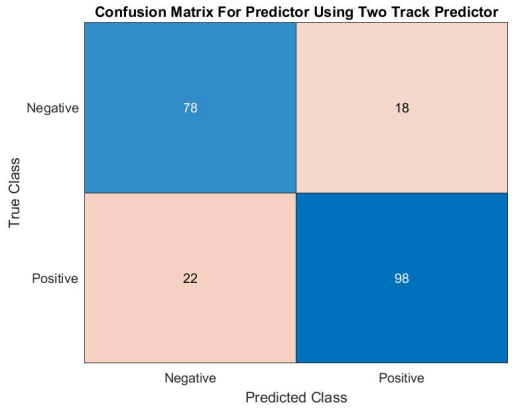

(b) Confusion matrix of the two-track predictor

Figure 4.9: Histogram of Δt_1 for cases when jackknifing occurs under varying predictor setup, initial velocity and F_{brake}^{req}.

and providing diminished lateral forces. By solely summing up the braking forces from the left and right wheel, the single-track model is unable to differentiate which wheel is losing the grip, leading to its incapability in effectively predicting jackknifing scenarios.

In contrast, the enhanced prediction capabilities of the two-track predictor can be attributed to its incorporation of both the longitudinal and lateral load transfers. This makes the two-track predictor gain a more comprehensive understanding of the dynamic changes during braking, particularly concerning the vertical forces on each wheel. The maximum contact force a tire can provide is linked to the vertical load F_Z on the tire. Vertical load F_Z is a key friction circle tire model component. In the single-track model, the vertical load F_Z on each wheel remains constant in calculating the lateral forces F_{yw}. Compared with the single-track model, the two-track

model considers the varied F_Z when determining lateral forces.

Both the single-track predictor and the two-track predictor have many true negative labels. The significant shortcoming of the predictor could be attributed to the limitations of the tire model employed in the motion model, combined with potential failures in the slip controller. The tire model cannot discern slip information, resulting in an inaccurate estimation of the lateral forces. This discrepancy leads to an overestimation of the lateral forces that can be supplied by the tires under high longitudinal slip conditions, ultimately misleading the predictor into perceiving the vehicle's stability as safer than it truly is.

Numerous tests include instances of slip controller failures, including the scenarios where the initial velocity is 40 km/h, $F_{brake}^{req} = -10000\text{N}, -20000\text{N}, -30000\text{N}$. And when velocity = 35 km/h, $F_{brake}^{req} = -20000\text{N}, -30000\text{N}$. The longitudinal slip becomes significant in these situations, leading to potential instances where the predictor fails to foresee potential jackknifing events. An illustrative case can be seen in Figure 4.10, where jackknifing arises due to the failure of the slip controller, leading to the lock of the wheels. Consequently, the locked wheel can provide limited lateral forces. The predictor fails to identify this perilous situation. As the VTM yaw rate difference increases, the predictor wrongly foresees a subsequent drop in the future yaw rate difference. This erroneous anticipation continues until the vehicle's state becomes a critical danger. Only at this late stage did the predictor finally acknowledge the instability.

In addition, in the case of the two-track predictor, the simplified roll dynamics within the two-track model can result in discrepancies within the vertical load obtained by the high-fidelity VTM model. Improving the modeling of roll dynamics could enhance the predictor's capability. Moreover, the prediction algorithm could be enhanced by incorporating a simplified slip controller to improve its capacity to foresee the input to the dynamic model.

4.4.1 Effectiveness of Trailer Braking Intervention in Preventing Jackknifing

For 120 instances of jackknifing with different predictor configurations, attempts were made to prevent jackknifing by applying trailer braking. Table 4.4 and Table 4.5 presents the effectiveness of the braking trailer.

The scenarios where successful prediction occurs but jackknifing prevention fails share a common characteristic. Specifically, these situations occur when the initial longitudinal speed $v_{x_0} = 43$ km/h. The failure cases are associated with a prediction horizon of 0.1 seconds when applying the two-track predictor. For the single-track predictor, jackknifing prevention failures extend beyond the cases with a 0.1 second prediction horizon, including instances of a 1 second prediction horizon. This observation indicates the inadequacy of a prediction horizon as short as 0.1 seconds for effective trailer braking intervention, even if the jackknifing is predicted in advance.

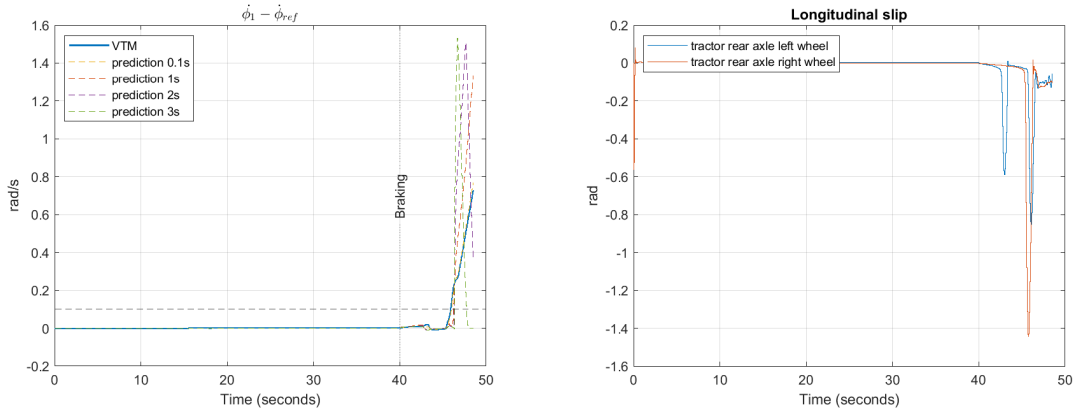

(a) Yaw rate difference **(b)** Longitudinal slip

Figure 4.10: Yaw rate difference and longitudinal slip on tractor rear axle for the case with 35 km/h velocity, a moderate braking $F_{brake}^{req} = -30000$ N. The predictor is configured with two-track model, $\tau_{pred} = 0.2$ and $F_{xwdesire} = F_{xw}^{act}$

In contrast, a prediction horizon of 1 second proves effective in jackknifing prevention for two-track predictor but not for single-track predictor.

There exist cases when the predictor fails to predict jackknifing in advance while the jackknifing is effectively prevented. These occurrences arise when the initial longitudinal speed is either $v_{x_0} = 35$ km/h or $v_{x_0} = 40$ km/h, and the longitudinal slip controller is not functioning well. For the two-track predictor, failure prediction but success prevention mainly happen when the prediction horizon is set to 0.1s. Similarly, the single-track predictor exhibits this pattern solely when the prediction horizon is also set as 0.1s.

Table 4.4: Braking trailer whether prevent jackknife or not - single track predictor

	Succeed to prevent jackknife	Fail to prevent jackknife
Succeed to predict ($\Delta t_1 < 0$)	74	18
Fail to predict ($\Delta t_1 \geq 0$)	1	27

Table 4.5: Braking trailer whether prevent jackknife or not - two track predictor

	Succeed to prevent jackknife	Fail to prevent jackknife
Succeed to predict ($\Delta t_1 < 0$)	86	12
Fail to predict ($\Delta t_1 \geq 0$)	13	9

4.5 Discussion

4.5.1 Testing cases

It can be observed that with the initial speeds $v_x = [35,\ 40]$ km/h, jackknifing only happens when the request braking force is strong, i.e., $F_{brake}^{req} = -30000$ N. When $v_x = 43$ km/h, jackknifing happens regardless of whether the braking force is gentle or strong. This observation highlights that jackknifing is influenced by both the steering angle and the magnitude of the braking force. Vehicles with increased steering angle in higher speed cases need additional lateral forces to maintain directional stability due to their high lateral acceleration. However, during braking, an increase in longitudinal slip could decrease the lateral forces supplied by the wheels, changing the yaw motion and potentially leading to jackknifing. On the other hand, vehicles with smaller lateral acceleration demand fewer lateral forces to maintain their directional stability, and therefore, stronger braking can be applied without encountering jackknifing.

Another risk factor leading to jackknifing during braking is the longitudinal load transfer, which causes a decreased axle load on the tractor's rear axle. As a result, the friction of the tractor's rear wheels decreases, decreasing the lateral forces that can be generated.

Finally, as the truck's speed decreases, lateral load transfer also diminishes. This leads to a reduction in the axle load on the outer wheels, decreasing the friction limit and the lateral forces of the outer wheels, which also increases the risk of jackknifing.

4.5.2 Prediction Horizon

An illustrative example that highlights the influence of predicted horizon length can be examined. In this scenario, the initial velocity is set at 40 km/h, and a strong braking $F_{brake}^{req} = -30000$ N is applied. The two-track predictor is involved, with $\tau_{pred} = 0.2$, and $F_{xwdesire} = F_{xw}^{act}$, the implication of varying predicted horizon $[0.1,\ 1,\ 2,\ 3]$s is investigated.

Figure 4.11 demonstrates the predicted yaw rate difference within this illustrative example, describing the impact of different prediction horizon lengths. With a shorter prediction horizon, the predictor forecasts the vehicle's dynamics in the very immediate future. Although this approach enables the predictor to provide immediate future vehicle dynamics that better approximate the vehicle's near future motion, it sacrifices the insight into the long-term trends, leading to delayed warnings of potential jackknifing compared with a longer predicted time length. Subsequently, this delayed warning combined with a deferred response of the trailer braking led to the failure of trailer braking to prevent jackknifing. On the contrary, using an extended predict horizon, such as 1 second, predicts the occurrence of jackknifing 1.41 second in advance, effectively preventing the jackknifing in this scenario.

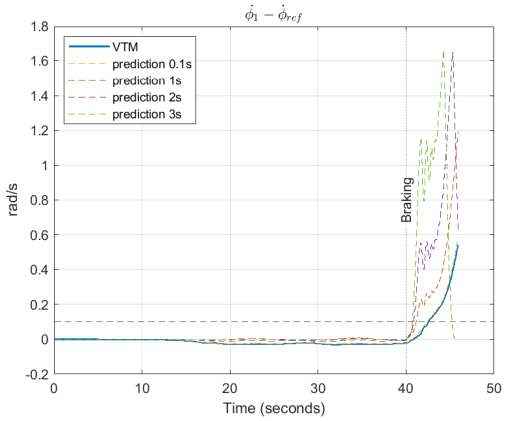

Figure 4.11: Yaw rate difference for the case with 43 km/h velocity, a gentle braking $F_{brake}^{req} = -10000$ N. The predictor is configured with two-track model, $\tau_{pred} = 0.2$ and $F_{xwdesire} = F_{xw}^{act}$.

On the other hand, a longer prediction horizon, such as 3 seconds, increases the possibility of false positive prediction. An example can be seen by considering the scenario when the initial velocity $v_{x0} = 40$ km/h, a moderate braking $F_{brake}^{req} = -20000$ N is applied. And the two-track predictor is engaged, with $\tau_{pred} = 0.2$, and $F_{xwdesire} = F_{xw}^{act}$, as shown in Figure 4.12. Although the predictor with a longer horizon provides an improved understanding of how the motion of the vehicle evolves over time, it is less responsive to rapid driver maneuvers changes occurring. As shown in Figure 4.12b, due to the intervention of the slip controller, which reduces the amount of the braking force on the tractor's rear left wheel around 41.6 seconds, the jackknifing situation is avoided. However, the predictor with the longer prediction horizon erroneously assumes future wheel forces and consequently predicts jackknifing.

These examples emphasize the importance of selecting an appropriate prediction time horizon to predict jackknifing. By comparing the predicted yaw rate difference using different prediction time horizons, we can conclude that the prolonged prediction horizon is less accurate in representing the future dynamics due to the lack of responsiveness to abrupt changes in driver input, thus leading to a driver input prediction with a large gap compared with the real driver input, and significantly increase the possibility of false predictions for jackknifing. Although a longer prediction horizon offers the advantage of better capturing the motion trends, it compromises the accuracy in predicting the motion due to the struggle in anticipating the future driver input. Among the four time horizons employed, a time horizon of 1 second exhibits better effectiveness than the other time horizons. It balances the ability to anticipate future motion trends while appropriately responding to sudden changes in driver input.

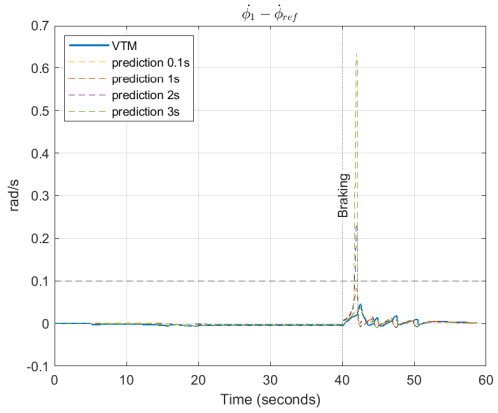

(a) Yaw rate difference

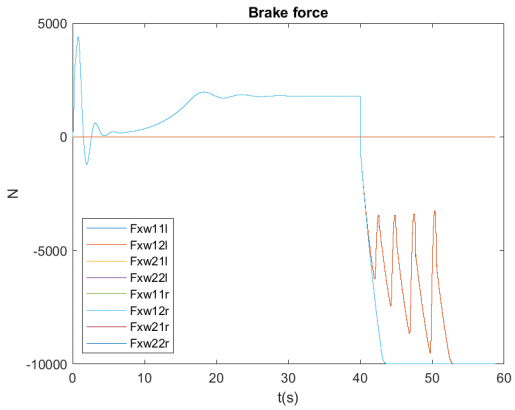

(b) Longitudinal force provided by the actuator

Figure 4.12: Yaw rate difference and longitudinal force input for the case with 40 km/h velocity, a moderate braking $F_{brake}^{req} = -20000$ N. The predictor is configured with two-track model, $\tau_{pred} = 0.2$ and $F_{xwdesire} = F_{xw}^{act}$

4.5.3 Selected Desired Force

Incorporating distinct desired forces provides valuable insights into predicting the future motion of the vehicle and potential jackknifing. By analyzing Figure 4.13, it indicates that these different desired forces exhibit little discrepancies under normal driving conditions, particularly when the slip controller does not intervene to moderate inner wheel slip by employing diminished braking forces in contrast to the requested braking forces.

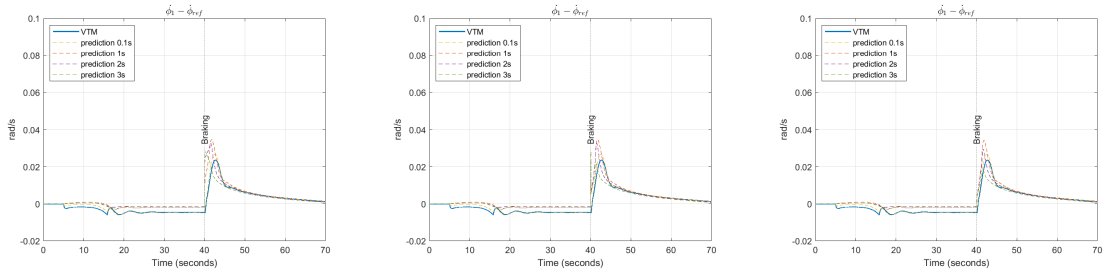

(a) Predicted yaw rate difference using F_{xw}^{req}

(b) Predicted yaw rate difference using F_{xw}^{ctrl}

(c) Predicted yaw rate difference using F_{xw}^{act}

Figure 4.13: Yaw rate difference for the case with 40 km/h velocity, a gentle braking $F_{brake}^{req} = -10000$ N. The predictor is configured with two-track model, $\tau_{pred} = 0.2$

Employing the desired force from the actuator acts the same as assuming the future braking forces remain constant. Employing desired forces from driver request and the slip controller offers distinct advantages over from the actuator in predicting jackknifing events. In test cases where the driver applies substantial force to the pedal (a significant driver requests braking forces), these input sources enhance the ability of the predictor to anticipate potential jackknifing occurrences compared

with using input from the actuator. This is exemplified by the relatively prompt jackknifing prediction immediately after the 40-second mark.

Adopting driver request and slip controller desired forces results in predictions characterized by a conservative approach. The conservativity arises from the acknowledgment that the force exerted by the actuator might not necessarily reach the desired values, which braking forces can be greater than the current actuator force in the upcoming moments. Consequently, relying on desired forces from both the slip controller and driver request enhances the predictor's ability to forecast jackknifing at an earlier stage. However, the increased conservatism also increases the likelihood of false positive predictions.

Comparatively, the distinctions between the outcomes obtained from the controller and the actuator are less pronounced during most of the time after the braking action. This similarity can be attributed to the close alignment between the forces stipulated by the controller and those from the actuator. A notable discrepancy arises at the initial phase of the braking when utilizing the desired force from the slip controller. This discrepancy can be attributed to the temporary match between the force value from the slip controller and the driver's requested value during the initial braking moments. Yet, this alignment does not guarantee that the actuator braking force will reach the driver's requested value during these brief moments.

In summary, using the desired forces from driver request forces and the slip controller values enhances the ability of the predictor to anticipate potential jackknifing, particularly when drivers apply substantial pedal force. Nevertheless, these approaches lead to more false positive predictions. On the other hand, the predicted motion using the controller and actuator inputs shows similar trends, except for an initial difference when using the slip controller's desired force. Generally, using the desired forces from the actuator yields better performance than the other two methods. The other two approaches may predict jackknifing at the beginning braking stage before the slip controller intervenes. As a result, they may overestimate the danger of jackknifing. However, despite the initial braking stage, using the desired force from the slip controller can still provide benefits in predicting jackknifing. This is because the current braking forces applied by the actuator could eventually reach the brake force specified by the slip controller in the future.

4.5.4 Driver Input Predictor Time Constant τ_{pred}

Using different predictor time constants causes no difference when the desired forces are from the actuator. Because this way assumes the future predicted driver braking forces will remain constant. However, the situation shifts when using desired forces from the slip controller or the driver request values. In scenarios with a shorter time constant $\tau_{pred} = 0.2$, the predictor tends to make an aggressive prediction regarding future driver maneuvers. This is due to the rapid transition of predicted future driver input from the actuator values to the desired values with a smaller time constant. While smaller time constants offer quicker reactions and provide jackknifing warnings

in earlier stages, they also can lead to more false positive predictions. Given that the truck is equipped with an actuator $\tau_{act} = 0.2$, it is advisable to maintain the same value when using τ_{pred} in the predictor.

5

Conclusion

Jackknifing is a severe yaw instability motion mode that poses a substantial danger in traffic situations. This thesis explores an innovative approach to address the issue of jackknifing instability for a specific tractor-semi-trailer combination. The proposed method can predict the motion and mitigate the occurrences of jackknifing for the proposed vehicle combination.

The study starts by modeling and assessing the accuracy of a single-track model and a two-track model with load transfer, analyzing the discrepancies of the above model compared with VTM. These models exhibit similarity in normal driving conditions. However, in severe cases, the single-track model fails to capture jackknifing events, while the two-track model is more sensitive to capture jackknifing than VTM. The main difference in dynamics described in the two-track model is caused by the implemented tire model, which is less advanced and more conservative in a low longitudinal slip condition than the Pacejka tire model utilized in VTM.

The developed prediction algorithms rely on a discrete state space model and driver input prediction techniques to foresee future motion. An innovative jackknifing indicator and a trailer braking strategy were established. These components construct a safety system to predict potential jackknifing events and enhance directional stability.

By exploring various driver input prediction techniques for the single-track and two-track models, the thesis finds longer prediction times, a 0.2s actuator time constant, and a preference for predicted future desired forces from slip controller and driver requested lead to conservative jackknifing predictions. However, the risk of false positive prediction is increased.

Generally, the predictor using the two-track model performs slightly better than the one based on the single-track model. Nonetheless, the predictor with either the single-track or two-track models exhibits reduced effectiveness for test cases when the slip controller fails to confine longitudinal slip. In scenarios involving high longitudinal slips, the limitations of the tire model become pronounced. This is because the friction ellipse model will produce more lateral force than the Pacejka model, which does not reflect conditions under high longitudinal slip conditions. Consequently, the timing of jackknifing predictions by the predictor tends to be delayed.

5.1 Future Work

While the thesis has demonstrated promising results in predicting and preventing jackknifing events for a specific tractor-semi-trailer combination, improvements and further research can be built based on the findings.

Advanced tire modeling can be beneficial for enhancing prediction accuracy. Employing tire models that better approximate real-world scenarios across a wide range of longitudinal slip conditions would be advantageous. Incorporating nonlinear factors such as temperature and tire pressure into the tire model could further improve the system's capability to anticipate jackknifing in various driving scenarios.

In addition, a more advanced jackknifing indicator threshold can be investigated. Although the current threshold is sufficiently high, it may not definitively indicate yaw instability and jackknifing occurrences in various driving situations. Parameters such as longitudinal velocity and steering angle should be considered when determining the threshold.

Bibliography

[1] Md Islam et al. *Design synthesis of articulated heavy vehicles with active trailer steering systems*. PhD thesis, 2010.

[2] M. F. J. Luijten. Lateral dynamic behaviour of articulated commercial vehicles. Master's thesis, Eindhoven University of Technology, 2010.

[3] M. Bouteldja and V. Cerezo. Jackknifing warning for articulated vehicles based on a detection and prediction system. In *Proceedings of the 3rd International Conference on Road Safety and Simulation*, Indianapolis, IN, September 2011.

[4] F. VLK. Lateral dynamics of commercial vehicle combinations: A literature survey. *Vehicle System Dynamics*, 11(5-6):305–324, 1982.

[5] Frank Hecker, Stefan Hurnrnel, Oliver Jundt, Klaus Leirnbach, et al. Vehicle dynamics control for commercial vehicles. *SAE Technical Paper*, (973284), 1997.

[6] Mehdi Abroshan, Reza Hajiloo, Ehsan Hashemi, and Amir Khajepour. Model predictive-based tractor-trailer stabilisation using differential braking with experimental verification. *Vehicle system dynamics*, 59(8):1190–1213, 2021.

[7] Mehdi Ahmadian. Integrating electromechanical systems in commercial vehicles for improved handling, stability, and comfort. *SAE International Journal of Commercial Vehicles*, 7(2014-01-2408):535–587, 2014.

[8] Amir Rahimi and Yuping He. A review of essential technologies for autonomous and semi-autonomous articulated heavy vehicles. In *Proceedings of the Canadian Society for Mechanical Engineering International Congress*, pages 21–24, 2020.

[9] Jere Lehtinen et al. Nonlinear lateral dynamic behavior of a high capacity transport vehicle. Master's thesis, 2015.

[10] International Organization for Standardization. Road vehicles — vehicle dynamics and road-holding ability — vocabulary. ISO 8855:2011, 2011.

[11] Umur Erdinc, Mats Jonasson, Maliheh Sadeghi Kati, Bengt Jacobson, Jonas Fredriksson, and Leo Laine. Safe operating envelope based on a single-track model for yaw instability avoidance of articulated heavy vehicles. 2023.

[12] Peter Nilsson and Kristoffer Tagesson. Single-track models of an a-double heavy vehicle combination. 2014.

[13] Toheed Ghandriz, Bengt Jacobson, Peter Nilsson, Leo Laine, and Niklas Fröjd. Computationally efficient nonlinear one- and two-track models for multitrailer road vehicles. *IEEE Access*, 8:203854–203875, 2020.

[14] P.S. Fancher. *Directional Dynamics Considerations for Multi-articulated, Multi-axled Heavy Vehicles*. S.A.E. technical papers. Society of Automotive Engineers, 1989.

[15] Bengt J H Jacobson, Mats Jonasson, and Fredrik Bruzelius. Compendium in vehicle motion engineering., 2022.
[16] Hans Pacejka and I. J. M. Besselink. *Tire and Vehicle Dynamics.* Elsevier Science Technology, 2012.
[17] Volvo 3P. VTM plant model description. 2018.
[18] Johan Hansson and Daniel Möller. Motion coordination of electric heavy vehicle combinations - maximizing regenerative braking during downhill coasting on low friction. Master's thesis, Chalmers University of Technology, Gothenburg, Sweden, 2022.
[19] Sebastien Gros with Bo Egardt. Modelling and simulation - Lecture notes for the Chalmers course ESS101, June 2021.
[20] Vincent Nguyen, Gregory Schultz, and Balakumar Balachandran. Lateral Load Transfer Effects on Bifurcation Behavior of Four-Wheel Vehicle System. *Journal of Computational and Nonlinear Dynamics*, 4(4):041007, 08 2009.
[21] MathWorks. matlabFunction - Convert symbolic expression to function handle or file.

A

Vehicle Parameters

Table A.1: Tractor semi-trailer parameters

Parameter	Tractor (Unit 1)	Semi-trailer (Unit 2)
m_i (kg)	6.9181×10^3	31000
I_{zi} (kg $\cdot$ m^2)	2.1237×10^4	4.6524×10^5
x_{aij} (m)	[0.9644, -2.7356]	[-1.5461, -2.8461]
x_{cij} (m)	[0, -2.1606]	[5.2539, 0]
t_{wij} (m)	[2.09, 1.85]	[2.05, 2.05]
h_i (m)	0.725	2.2724
h_{cij} (m)	[0, 1.1230]	[1.1230, 0.5]
h_{r1j} (m)	[0.4550, 0.8700]	/
c_{r1j} (m)	[0.3086×10^6, 0.4982×10^6]	/
F_{z0ijk} (N)	$F_{z011l} = F_{z011r} = \frac{64108.6}{2}$ $F_{z012l} = F_{z012r} = \frac{93403.1}{2}$	$F_{z021l} = F_{z021r} = \frac{214465}{4}$ $F_{z022l} = F_{z022r} = \frac{214465}{4}$
c_{yijk}	$c_{y11l} = c_{y11r}$ = -5.8860 $c_{y12l} = c_{y12r}$ = -5.9880	$c_{y21l} = c_{y21r}$ = -5.4655 $c_{y22l} = c_{y22r}$ = -5.4575
r_i (m)	5.0924×10^{-1}	5.3424×10^{-1}

Table A.2: Physical parameters

μ	g (m/s^2)	A_f (m^2)	c_d	ρ_{air} (kg/m^3)	f_r
0.3	9.81	5.2	1	1.2	0

B

Prediction Results

B.1 Results of Single-track Predictor

B.1.1 Non-jackknife Cases - VTM t_0 Does Not Exist

Table B.1: v_{x0} = 35km/h, sample time = 0.01s

Total request brake force (N)	τ_{pred}	Desired Force	Predict Horizon	Predict t_1 (s)	Predict t_2 (s)	Δt_1 (s)	Δt_2 (s)	Action prevent jackknife
10000	0.2	Request	0.1s	\	\	\	\	Inactive
10000	0.2	Request	1s	\	\	\	\	Inactive
10000	0.2	Request	2s	\	\	\	\	Inactive
10000	0.2	Request	3s	\	\	\	\	Inactive
10000	0.2	Controller	0.1s	\	\	\	\	Inactive
10000	0.2	Controller	1s	\	\	\	\	Inactive
10000	0.2	Controller	2s	\	\	\	\	Inactive
10000	0.2	Controller	3s	\	\	\	\	Inactive
10000	0.2	Actuator	0.1s	\	\	\	\	Inactive
10000	0.2	Actuator	1s	\	\	\	\	Inactive
10000	0.2	Actuator	2s	\	\	\	\	Inactive
10000	0.2	Actuator	3s	\	\	\	\	Inactive
10000	1	Request	0.1s	\	\	\	\	Inactive
10000	1	Request	1s	\	\	\	\	Inactive
10000	1	Request	2s	\	\	\	\	Inactive
10000	1	Request	3s	\	\	\	\	Inactive
10000	1	Controller	0.1s	\	\	\	\	Inactive
10000	1	Controller	1s	\	\	\	\	Inactive
10000	1	Controller	2s	\	\	\	\	Inactive
10000	1	Controller	3s	\	\	\	\	Inactive
10000	1	Actuator	0.1s	\	\	\	\	Inactive
10000	1	Actuator	1s	\	\	\	\	Inactive
10000	1	Actuator	2s	\	\	\	\	Inactive
10000	1	Actuator	3s	\	\	\	\	Inactive

20000	0.2	Request	0.1s	\	\	\	\	Inactive
20000	0.2	Request	1s	\	\	\	\	Inactive
20000	0.2	Request	2s	\	\	\	\	Inactive
20000	0.2	Request	3s	\	\	\	\	Inactive
20000	0.2	Controller	0.1s	\	\	\	\	Inactive
20000	0.2	Controller	1s	\	\	\	\	Inactive
20000	0.2	Controller	2s	\	\	\	\	Inactive
20000	0.2	Controller	3s	\	\	\	\	Inactive
20000	0.2	Actuator	0.1s	\	\	\	\	Inactive
20000	0.2	Actuator	1s	\	\	\	\	Inactive
20000	0.2	Actuator	2s	\	\	\	\	Inactive
20000	0.2	Actuator	3s	\	\	\	\	Inactive
20000	1	Request	0.1s	\	\	\	\	Inactive
20000	1	Request	1s	\	\	\	\	Inactive
20000	1	Request	2s	\	\	\	\	Inactive
20000	1	Request	3s	\	\	\	\	Inactive
20000	1	Controller	0.1s	\	\	\	\	Inactive
20000	1	Controller	1s	\	\	\	\	Inactive
20000	1	Controller	2s	\	\	\	\	Inactive
20000	1	Controller	3s	\	\	\	\	Inactive
20000	1	Actuator	0.1s	\	\	\	\	Inactive
20000	1	Actuator	1s	\	\	\	\	Inactive
20000	1	Actuator	2s	\	\	\	\	Inactive
20000	1	Actuator	3s	\	\	\	\	Inactive

Table B.2: v_{x0} = 40km/h, sample time = 0.01s

Total request brake force (N)	τ_{pred}	Desired Force	Predict Hori-zon	Predict t_1 (s)	Predict t_2 (s)	Δt_1 (s)	Δt_2 (s)	Action prevent jack-knife
10000	0.2	Request	1s	\	\	\	\	Inactive
10000	0.2	Request	2s	\	\	\	\	Inactive
10000	0.2	Request	3s	\	\	\	\	Inactive
10000	0.2	Controller	0.1s	\	\	\	\	Inactive
10000	0.2	Controller	1s	\	\	\	\	Inactive
10000	0.2	Controller	2s	\	\	\	\	Inactive
10000	0.2	Controller	3s	\	\	\	\	Inactive
10000	0.2	Actuator	0.1s	\	\	\	\	Inactive
10000	0.2	Actuator	1s	\	\	\	\	Inactive
10000	0.2	Actuator	2s	\	\	\	\	Inactive
10000	0.2	Actuator	3s	\	\	\	\	Inactive
10000	1	Request	0.1s	\	\	\	\	Inactive

10000	1	Request	1s	\	\	\	\	Inactive
10000	1	Request	2s	\	\	\	\	Inactive
10000	1	Request	3s	\	\	\	\	Inactive
10000	1	Controller	0.1s	\	\	\	\	Inactive
10000	1	Controller	1s	\	\	\	\	Inactive
10000	1	Controller	2s	\	\	\	\	Inactive
10000	1	Controller	3s	\	\	\	\	Inactive
10000	1	Actuator	0.1s	\	\	\	\	Inactive
10000	1	Actuator	1s	\	\	\	\	Inactive
10000	1	Actuator	2s	\	\	\	\	Inactive
10000	1	Actuator	3s	\	\	\	\	Inactive
20000	0.2	Request	0.1s	\	\	\	\	Inactive
20000	0.2	Request	1s	42.34	42.34	$\sim$	$\sim$	Success
20000	0.2	Request	2s	40.02	40.02	$\sim$	$\sim$	Success
20000	0.2	Request	3s	40.02	40.02	$\sim$	$\sim$	Success
20000	0.2	Controller	0.1s	\	\	\	\	Inactive
20000	0.2	Controller	1s	\	\	\	\	Inactive
20000	0.2	Controller	2s	40.01	40.01	$\sim$	$\sim$	Success
20000	0.2	Controller	3s	40.01	40.01	$\sim$	$\sim$	Success
20000	0.2	Actuator	0.1s	\	\	\	\	Inactive
20000	0.2	Actuator	1s	\	\	\	\	Inactive
20000	0.2	Actuator	2s	\	\	\	\	Inactive
20000	0.2	Actuator	3s	\	\	\	\	Inactive
20000	1	Request	0.1s	\	\	\	\	Inactive
20000	1	Request	1s	\	\	\	\	Inactive
20000	1	Request	2s	\	\	\	\	Inactive
20000	1	Request	3s	\	\	\	\	Inactive
20000	1	Controller	0.1s	\	\	\	\	Inactive
20000	1	Controller	1s	\	\	\	\	Inactive
20000	1	Controller	2s	\	\	\	\	Inactive
20000	1	Controller	3s	\	\	\	\	Inactive
20000	1	Actuator	0.1s	\	\	\	\	Inactive
20000	1	Actuator	1s	\	\	\	\	Inactive
20000	1	Actuator	2s	\	\	\	\	Inactive
20000	1	Actuator	3s	\	\	\	\	Inactive

B.1.2 Jackknife Cases

Table B.3: v_{x0} = 35km/h, F_{brake}^{req} = -30000N, VTM t_0 = 45.89s, sample time = 0.01s

Total request brake force (N)	τ_{pred}	Desired Force	Predict Horizon	Predict t_1 (s)	Predict t_2 (s)	Δt_1 (s)	Δt_2 (s)	Action prevent jack-knife
30000	0.2	Request	0.1s	45.98	45.98	0.09	0.09	Fail
30000	0.2	Request	1s	40.02	40.02	-5.87	-5.87	Success
30000	0.2	Request	2s	40.02	40.02	-5.87	-5.87	Success
30000	0.2	Request	3s	40.02	47.47	-5.87	1.58	Success
30000	0.2	Controller	0.1s	46	46	0.11	0.11	Fail
30000	0.2	Controller	1s	40.01	46.22	-5.88	0.33	Success
30000	0.2	Controller	2s	40.01	46.28	-5.88	0.39	Success
30000	0.2	Controller	3s	40.01	46.28	-5.88	0.39	Success
30000	0.2	Actuator	0.1s	46	46	0.11	0.11	Fail
30000	0.2	Actuator	1s	46.23	46.23	0.34	0.34	Fail
30000	0.2	Actuator	2s	46.3	46.3	0.41	0.41	Fail
30000	0.2	Actuator	3s	46.33	46.33	0.44	0.44	Fail
30000	1	Request	0.1s	45.99	45.99	0.1	0.1	Fail
30000	1	Request	1s	46.13	46.13	0.24	0.24	Fail
30000	1	Request	2s	40.04	46.11	-5.85	0.22	Success
30000	1	Request	3s	40.02	45.87	-5.87	-0.02	Success
30000	1	Controller	0.1s	46	46	0.11	0.11	Fail
30000	1	Controller	1s	46.23	46.23	0.34	0.34	Fail
30000	1	Controller	2s	46.28	46.28	0.39	0.39	Fail
30000	1	Controller	3s	40.01	46.28	-5.88	0.39	Success
30000	1	Actuator	0.1s	46	46	0.11	0.11	Fail
30000	1	Actuator	1s	46.23	46.23	0.34	0.34	Fail
30000	1	Actuator	2s	46.3	46.3	0.41	0.41	Fail
30000	1	Actuator	3s	46.33	46.33	0.44	0.44	Fail

Table B.4: v_{x0} = 40km/h, F_{brake}^{req} = -30000N, VTM t_0 = 46.24s, sample time = 0.01s

Total request brake force (N)	τ_{pred}	Desired Force	Predict Horizon	Predict t_1 (s)	Predict t_2 (s)	Δt_1 (s)	Δt_2 (s)	Action prevent jack-knife
30000	0.2	Request	0.1s	46.29	46.29	0.05	0.05	Success
30000	0.2	Request	1s	40.02	40.02	-6.22	-6.22	Success
30000	0.2	Request	2s	40.02	40.02	-6.22	-6.22	Success
30000	0.2	Request	3s	40.02	40.02	-6.22	-6.22	Success
30000	0.2	Controller	0.1s	46.32	46.32	0.08	0.08	Fail
30000	0.2	Controller	1s	40.01	46.47	-6.23	0.23	Success

30000	0.2	Controller	2s	40.01	46.5	-6.23	0.26	Success
30000	0.2	Controller	3s	40.01	46.51	-6.23	0.27	Success
30000	0.2	Actuator	0.1s	46.32	46.32	0.08	0.08	Fail
30000	0.2	Actuator	1s	46.45	46.45	0.21	0.21	Fail
30000	0.2	Actuator	2s	46.48	46.48	0.24	0.24	Fail
30000	0.2	Actuator	3s	46.5	46.5	0.26	0.26	Fail
30000	1	Request	0.1s	46.32	46.32	0.08	0.08	Fail
30000	1	Request	1s	41.73	46.3	-4.51	0.06	Success
30000	1	Request	2s	40.02	40.02	-6.22	-6.22	Success
30000	1	Request	3s	40.02	40.02	-6.22	-6.22	Success
30000	1	Controller	0.1s	46.32	46.32	0.08	0.08	Fail
30000	1	Controller	1s	46.46	46.46	0.22	0.22	Fail
30000	1	Controller	2s	40.01	46.49	-6.23	0.25	Success
30000	1	Controller	3s	40.01	46.5	-6.23	0.26	Success
30000	1	Actuator	0.1s	46.32	46.32	0.08	0.08	Fail
30000	1	Actuator	1s	46.45	46.45	0.21	0.21	Fail
30000	1	Actuator	2s	46.48	46.48	0.24	0.24	Fail
30000	1	Actuator	3s	46.49	46.49	0.25	0.25	Fail

Table B.5: v_{x0} = 43km/h, F_{brake}^{req} = -10000N, VTM t_0 = 42.55s, sample time = 0.01s

Total request brake force (N)	τ_{pred}	Desired Force	Predict Horizon	Predict t_1 (s)	Predict t_2 (s)	Δt_1 (s)	Δt_2 (s)	Action prevent jack-knife
10000	0.2	Request	0.1s	42.48	42.48	-0.07	-0.07	Fail
10000	0.2	Request	1s	41.73	41.73	-0.82	-0.82	Fail
10000	0.2	Request	2s	41.05	41.05	-1.5	-1.5	Success
10000	0.2	Request	3s	40.02	40.02	-2.53	-2.53	Success
10000	0.2	Controller	0.1s	42.49	42.49	-0.06	-0.06	Fail
10000	0.2	Controller	1s	41.84	41.84	-0.71	-0.71	Fail
10000	0.2	Controller	2s	41.22	41.22	-1.33	-1.33	Success
10000	0.2	Controller	3s	40.01	41.1	-2.54	-1.45	Success
10000	0.2	Actuator	0.1s	42.49	42.49	-0.06	-0.06	Fail
10000	0.2	Actuator	1s	41.76	41.76	-0.79	-0.79	Fail
10000	0.2	Actuator	2s	41.35	41.35	-1.2	-1.2	Success
10000	0.2	Actuator	3s	41.24	41.24	-1.31	-1.31	Success
10000	1	Request	0.1s	42.49	42.49	-0.06	-0.06	Fail
10000	1	Request	1s	41.74	41.74	-0.81	-0.81	Fail
10000	1	Request	2s	41.25	41.25	-1.3	-1.3	Success
10000	1	Request	3s	40.99	40.99	-1.56	-1.56	Success
10000	1	Controller	0.1s	42.49	42.49	-0.06	-0.06	Fail

10000	1	Controller	1s	41.8	41.8	-0.75	-0.75	Fail
10000	1	Controller	2s	41.28	41.28	-1.27	-1.27	Success
10000	1	Controller	3s	41.15	41.15	-1.4	-1.4	Success
10000	1	Actuator	0.1s	42.49	42.49	-0.06	-0.06	Fail
10000	1	Actuator	1s	41.76	41.76	-0.79	-0.79	Fail
10000	1	Actuator	2s	41.35	41.35	-1.2	-1.2	Success
10000	1	Actuator	3s	41.24	41.24	-1.31	-1.31	Success

Table B.6: v_{x0} = 43km/h, F_{brake}^{req} = -20000N, VTM t_0 = 43.4s, sample time = 0.01s

Total request brake force (N)	τ_{pred}	Desired Force	Predict Horizon	Predict t_1 (s)	Predict t_2 (s)	Δt_1 (s)	Δt_2 (s)	Action prevent jack-knife
20000	0.2	Request	0.1s	43.26	43.26	-0.14	-0.14	Fail
20000	0.2	Request	1s	40.02	40.02	-3.38	-3.38	Success
20000	0.2	Request	2s	40.02	40.02	-3.38	-3.38	Success
20000	0.2	Request	3s	40.02	40.02	-3.38	-3.38	Success
20000	0.2	Controller	0.1s	43.3	43.3	-0.1	-0.1	Fail
20000	0.2	Controller	1s	40.01	41.58	-3.39	-1.82	Success
20000	0.2	Controller	2s	40.01	41.04	-3.39	-2.36	Success
20000	0.2	Controller	3s	40.01	40.9	-3.39	-2.5	Success
20000	0.2	Actuator	0.1s	43.29	43.29	-0.11	-0.11	Fail
20000	0.2	Actuator	1s	41.51	41.51	-1.89	-1.89	Success
20000	0.2	Actuator	2s	41.16	41.16	-2.24	-2.24	Success
20000	0.2	Actuator	3s	41.05	41.05	-2.35	-2.35	Success
20000	1	Request	0.1s	43.29	43.29	-0.11	-0.11	Fail
20000	1	Request	1s	41.05	41.05	-2.35	-2.35	Success
20000	1	Request	2s	40.02	40.02	-3.38	-3.38	Success
20000	1	Request	3s	40.02	40.02	-3.38	-3.38	Success
20000	1	Controller	0.1s	43.3	43.3	-0.1	-0.1	Fail
20000	1	Controller	1s	41.5	41.5	-1.9	-1.9	Success
20000	1	Controller	2s	40.01	41.09	-3.39	-2.31	Success
20000	1	Controller	3s	40.01	40.96	-3.39	-2.44	Success
20000	1	Actuator	0.1s	43.29	43.29	-0.11	-0.11	Fail
20000	1	Actuator	1s	41.51	41.51	-1.89	-1.89	Success
20000	1	Actuator	2s	41.16	41.16	-2.24	-2.24	Success
20000	1	Actuator	3s	41.05	41.05	-2.35	-2.35	Success

Table B.7: v_{x0} = 43km/h, F_{brake}^{req} = -30000N, VTM t_0 = 43.36s, sample time = 0.01s

Total request brake force (N)	τ_{pred}	Desired Force	Predict Horizon	Predict t_1 (s)	Predict t_2 (s)	Δt_1 (s)	Δt_2 (s)	Action prevent jack-knife
30000	0.2	Request	0.1s	43.15	43.15	-0.21	-0.21	Success
30000	0.2	Request	1s	40.02	40.02	-3.34	-3.34	Success
30000	0.2	Request	2s	40.02	40.02	-3.34	-3.34	Success
30000	0.2	Request	3s	40.02	40.02	-3.34	-3.34	Success
30000	0.2	Controller	0.1s	43.26	43.26	-0.1	-0.1	Success
30000	0.2	Controller	1s	40.01	41.53	-3.35	-1.83	Success
30000	0.2	Controller	2s	40.01	40.99	-3.35	-2.37	Success
30000	0.2	Controller	3s	40.01	40.84	-3.35	-2.52	Success
30000	0.2	Actuator	0.1s	43.25	43.25	-0.11	-0.11	Success
30000	0.2	Actuator	1s	41.16	41.16	-2.2	-2.2	Success
30000	0.2	Actuator	2s	41.11	41.11	-2.25	-2.25	Success
30000	0.2	Actuator	3s	41.1	41.1	-2.26	-2.26	Success
30000	1	Request	0.1s	43.24	43.24	-0.12	-0.12	Success
30000	1	Request	1s	40.32	40.32	-3.04	-3.04	Success
30000	1	Request	2s	40.02	40.02	-3.34	-3.34	Success
30000	1	Request	3s	40.02	40.02	-3.34	-3.34	Success
30000	1	Controller	0.1s	43.25	43.25	-0.11	-0.11	Success
30000	1	Controller	1s	41.45	41.45	-1.91	-1.91	Success
30000	1	Controller	2s	40.01	41.04	-3.35	-2.32	Success
30000	1	Controller	3s	40.01	40.9	-3.35	-2.46	Success
30000	1	Actuator	0.1s	43.25	43.25	-0.11	-0.11	Success
30000	1	Actuator	1s	41.46	41.46	-1.9	-1.9	Success
30000	1	Actuator	2s	41.11	41.11	-2.25	-2.25	Success
30000	1	Actuator	3s	41	41	-2.36	-2.36	Success

B.2 Results of Two Track Predictor

B.2.1 Non-jackknife Cases - VTM t_0 Does Not Exist

Table B.8: v_{x0} = 35km/h, sample time = 0.01s

Total request brake force (N)	τ_{pred}	Desired Force	Predict Horizon	Predict t_1 (s)	Predict t_2 (s)	Δt_1 (s)	Δt_2 (s)	Action prevent jack-knife
10000	0.2	Request	0.1s	\	\	\	\	Inactive
10000	0.2	Request	1s	\	\	\	\	Inactive

10000	0.2	Request	2s	\	\	\	\	Inactive
10000	0.2	Request	3s	\	\	\	\	Inactive
10000	0.2	Controller	0.1s	\	\	\	\	Inactive
10000	0.2	Controller	1s	\	\	\	\	Inactive
10000	0.2	Controller	2s	\	\	\	\	Inactive
10000	0.2	Controller	3s	\	\	\	\	Inactive
10000	0.2	Actuator	0.1s	\	\	\	\	Inactive
10000	0.2	Actuator	1s	\	\	\	\	Inactive
10000	0.2	Actuator	2s	\	\	\	\	Inactive
10000	0.2	Actuator	3s	\	\	\	\	Inactive
10000	1	Request	0.1s	\	\	\	\	Inactive
10000	1	Request	1s	\	\	\	\	Inactive
10000	1	Request	2s	\	\	\	\	Inactive
10000	1	Request	3s	\	\	\	\	Inactive
10000	1	Controller	0.1s	\	\	\	\	Inactive
10000	1	Controller	1s	\	\	\	\	Inactive
10000	1	Controller	2s	\	\	\	\	Inactive
10000	1	Controller	3s	\	\	\	\	Inactive
10000	1	Actuator	0.1s	\	\	\	\	Inactive
10000	1	Actuator	1s	\	\	\	\	Inactive
10000	1	Actuator	2s	\	\	\	\	Inactive
10000	1	Actuator	3s	\	\	\	\	Inactive
20000	0.2	Request	0.1s	\	\	\	\	Inactive
20000	0.2	Request	1s	\	\	\	\	Inactive
20000	0.2	Request	2s	40.01	40.01	$\sim$	$\sim$	Success
20000	0.2	Request	3s	40.01	40.01	$\sim$	$\sim$	Success
20000	0.2	Controller	0.1s	\	\	\	\	Inactive
20000	0.2	Controller	1s	\	\	\	\	Inactive
20000	0.2	Controller	2s	40.01	40.01	$\sim$	$\sim$	Success
20000	0.2	Controller	3s	40.01	40.01	$\sim$	$\sim$	Success
20000	0.2	Actuator	0.1s	\	\	\	\	Inactive
20000	0.2	Actuator	1s	\	\	\	\	Inactive
20000	0.2	Actuator	2s	\	\	\	\	Inactive
20000	0.2	Actuator	3s	\	\	\	\	Inactive
20000	1	Request	0.1s	\	\	\	\	Inactive
20000	1	Request	1s	\	\	\	\	Inactive
20000	1	Request	2s	\	\	\	\	Inactive
20000	1	Request	3s	\	\	\	\	Inactive
20000	1	Controller	0.1s	\	\	\	\	Inactive
20000	1	Controller	1s	\	\	\	\	Inactive
20000	1	Controller	2s	\	\	\	\	Inactive
20000	1	Controller	3s	\	\	\	\	Inactive
20000	1	Actuator	0.1s	\	\	\	\	Inactive
20000	1	Actuator	1s	\	\	\	\	Inactive

20000	1	Actuator	2s	\	\	\	\	Inactive
20000	1	Actuator	3s	\	\	\	\	Inactive

Table B.9: v_{x0} = 40km/h, sample time = 0.01s

Total request brake force (N)	τ_{pred}	Desired Force	Predict Hori-zon	Predict t_1 (s)	Predict t_2 (s)	Δt_1 (s)	Δt_2 (s)	Action prevent jack-knife
10000	0.2	Request	0.1s	\	\	\	\	Inactive
10000	0.2	Request	1s	\	\	\	\	Inactive
10000	0.2	Request	2s	\	\	\	\	Inactive
10000	0.2	Request	3s	\	\	\	\	Inactive
10000	0.2	Controller	0.1s	\	\	\	\	Inactive
10000	0.2	Controller	1s	\	\	\	\	Inactive
10000	0.2	Controller	2s	\	\	\	\	Inactive
10000	0.2	Controller	3s	\	\	\	\	Inactive
10000	0.2	Actuator	0.1s	\	\	\	\	Inactive
10000	0.2	Actuator	1s	\	\	\	\	Inactive
10000	0.2	Actuator	2s	\	\	\	\	Inactive
10000	0.2	Actuator	3s	\	\	\	\	Inactive
10000	1	Request	0.1s	\	\	\	\	Inactive
10000	1	Request	1s	\	\	\	\	Inactive
10000	1	Request	2s	\	\	\	\	Inactive
10000	1	Request	3s	\	\	\	\	Inactive
10000	1	Controller	0.1s	\	\	\	\	Inactive
10000	1	Controller	1s	\	\	\	\	Inactive
10000	1	Controller	2s	\	\	\	\	Inactive
10000	1	Controller	3s	\	\	\	\	Inactive
10000	1	Actuator	0.1s	\	\	\	\	Inactive
10000	1	Actuator	1s	\	\	\	\	Inactive
10000	1	Actuator	2s	\	\	\	\	Inactive
10000	1	Actuator	3s	\	\	\	\	Inactive
20000	0.2	Request	0.1s	\	\	\	\	Inactive
20000	0.2	Request	1s	40.78	$\sim$	$\sim$	$\sim$	Success
20000	0.2	Request	2s	40.01	$\sim$	$\sim$	$\sim$	Success
20000	0.2	Request	3s	40.01	$\sim$	$\sim$	$\sim$	Success
20000	0.2	Controller	0.1s	\	\	\	\	Inactive
20000	0.2	Controller	1s	\	\	\	\	Inactive
20000	0.2	Controller	2s	40.01	$\sim$	$\sim$	$\sim$	Success
20000	0.2	Controller	3s	40.01	$\sim$	$\sim$	$\sim$	Success
20000	0.2	Actuator	0.1s	\	\	\	\	Inactive
20000	0.2	Actuator	1s	\	\	\	\	Inactive

20000	0.2	Actuator	2s	41.72	∼	∼	∼	Success
20000	0.2	Actuator	3s	41.65	∼	∼	∼	Success
20000	1	Request	0.1s	\	\	\	\	Inactive
20000	1	Request	1s	41.22	∼	∼	∼	Success
20000	1	Request	2s	40.01	∼	∼	∼	Success
20000	1	Request	3s	40.01	∼	∼	∼	Success
20000	1	Controller	0.1s	\	\	\	\	Inactive
20000	1	Controller	1s	\	\	\	\	Inactive
20000	1	Controller	2s	40.01	∼	∼	∼	Success
20000	1	Controller	3s	40.01	∼	∼	∼	Success
20000	1	Actuator	0.1s	\	\	\	\	Inactive
20000	1	Actuator	1s	\	\	\	\	Inactive
20000	1	Actuator	2s	41.72	∼	∼	∼	Success
20000	1	Actuator	3s	41.65	∼	∼	∼	Success

B.2.2 Jackknife Cases

Table B.10: v_{x0} = 35km/h, F_{brake}^{req} = -30000N, VTM t_0 = 45.89s, sample time = 0.01s

Total request brake force (N)	τ_{pred}	Desired Force	Predict Horizon	Predict t_1 (s)	Predict t_2 (s)	Δt_1 (s)	Δt_2 (s)	Action prevent jackknife
30000	0.2	Request	0.1s	45.93	45.93	0.04	0.04	Success
30000	0.2	Request	1s	45.83	45.83	-0.06	-0.06	Success
30000	0.2	Request	2s	40.01	45.75	-5.88	-0.14	Success
30000	0.2	Request	3s	40.01	45.71	-5.88	-0.18	Success
30000	0.2	Controller	0.1s	45.97	45.97	0.08	0.08	Success
30000	0.2	Controller	1s	46.22	46.22	0.33	0.33	Fail
30000	0.2	Controller	2s	40.01	46.31	-5.88	0.42	Success
30000	0.2	Controller	3s	40.01	46.27	-5.88	0.38	Success
30000	0.2	Actuator	0.1s	45.98	45.98	0.09	0.09	Success
30000	0.2	Actuator	1s	46.2	46.2	0.31	0.31	Fail
30000	0.2	Actuator	2s	46.3	46.3	0.41	0.41	Fail
30000	0.2	Actuator	3s	46.33	46.33	0.44	0.44	Fail
30000	1	Request	0.1s	45.96	45.96	0.07	0.07	Success
30000	1	Request	1s	46.04	46.04	0.15	0.15	Success
30000	1	Request	2s	46.05	46.05	0.16	0.16	Success
30000	1	Request	3s	40.01	46.05	-5.88	0.16	Success
30000	1	Controller	0.1s	45.97	45.97	0.08	0.08	Success
30000	1	Controller	1s	46.21	46.21	0.32	0.32	Fail
30000	1	Controller	2s	46.27	46.27	0.38	0.38	Fail

30000	1	Controller	3s	40.01	46.28	-5.88	0.39	Success
30000	1	Actuator	0.1s	45.97	45.97	0.08	0.08	Success
30000	1	Actuator	1s	46.2	46.2	0.31	0.31	Fail
30000	1	Actuator	2s	46.3	46.3	0.41	0.41	Fail
30000	1	Actuator	3s	46.33	46.33	0.44	0.44	Fail

Table B.11: v_{x0} = 40km/h, F_{brake}^{req} = -30000N, VTM t_0 = 46.24s, sample time = 0.01s

Total request brake force (N)	τ_{pred}	Desired Force	Predict Horizon	Predict t_1 (s)	Predict t_2 (s)	Δt_1 (s)	Δt_2 (s)	Action prevent jack-knife
30000	0.2	Request	0.1s	46.22	46.22	-0.02	-0.02	Success
30000	0.2	Request	1s	40.24	45.94	-6	-0.3	Success
30000	0.2	Request	2s	40.01	40.01	-6.23	-6.23	Success
30000	0.2	Request	3s	40.01	40.01	-6.23	-6.23	Success
30000	0.2	Controller	0.1s	46.25	46.25	0.01	0.01	Success
30000	0.2	Controller	1s	41.73	46.2	-4.51	-0.04	Success
30000	0.2	Controller	2s	40.01	46.2	-6.23	-0.04	Success
30000	0.2	Controller	3s	40.01	46.19	-6.23	-0.05	Success
30000	0.2	Actuator	0.1s	46.25	46.25	0.01	0.01	Success
30000	0.2	Actuator	1s	46.23	46.23	-0.01	-0.01	Success
30000	0.2	Actuator	2s	41.58	46.23	-4.66	-0.01	Success
30000	0.2	Actuator	3s	41.51	46.23	-4.73	-0.01	Success
30000	1	Request	0.1s	46.24	46.24	0	0	Success
30000	1	Request	1s	40.89	46.1	-5.35	-0.14	Success
30000	1	Request	2s	40.01	46.03	-6.23	-0.21	Success
30000	1	Request	3s	40.01	46	-6.23	-0.24	Success
30000	1	Controller	0.1s	46.25	46.25	0.01	0.01	Success
30000	1	Controller	1s	46.22	46.22	-0.02	-0.02	Success
30000	1	Controller	2s	40.01	46.22	-6.23	-0.02	Success
30000	1	Controller	3s	40.01	46.21	-6.23	-0.03	Success
30000	1	Actuator	0.1s	46.25	46.25	0.01	0.01	Success
30000	1	Actuator	1s	46.23	46.23	-0.01	-0.01	Success
30000	1	Actuator	2s	41.58	46.23	-4.66	-0.01	Success
30000	1	Actuator	3s	41.51	46.23	-4.73	-0.01	Success

Table B.12: v_{x0} = 43km/h, F_{brake}^{req} = -10000N, VTM t_0 = 42.55s, sample time = 0.01s

Total request brake force (N)	τ_{pred}	Desired Force	Predict Horizon	Predict t_1 (s)	Predict t_2 (s)	Δt_1 (s)	Δt_2 (s)	Action prevent jack-knife
10000	0.2	Request	0.1s	42.41	42.41	-0.14	-0.14	Fail
10000	0.2	Request	1s	40.34	40.34	-2.21	-2.21	Success
10000	0.2	Request	2s	40.01	40.01	-2.54	-2.54	Success
10000	0.2	Request	3s	40.01	40.01	-2.54	-2.54	Success
10000	0.2	Controller	0.1s	42.45	42.45	-0.1	-0.1	Fail
10000	0.2	Controller	1s	41.03	41.03	-1.52	-1.52	Success
10000	0.2	Controller	2s	40.01	40.67	-2.54	-1.88	Success
10000	0.2	Controller	3s	40.01	40.51	-2.54	-2.04	Success
10000	0.2	Actuator	0.1s	42.43	42.43	-0.12	-0.12	Fail
10000	0.2	Actuator	1s	41.14	41.14	-1.41	-1.41	Success
10000	0.2	Actuator	2s	40.84	40.84	-1.71	-1.71	Success
10000	0.2	Actuator	3s	40.71	40.71	-1.84	-1.84	Success
10000	1	Request	0.1s	42.43	42.43	-0.12	-0.12	Fail
10000	1	Request	1s	40.98	40.98	-1.57	-1.57	Success
10000	1	Request	2s	40.08	40.08	-2.47	-2.47	Success
10000	1	Request	3s	40.01	40.01	-2.54	-2.54	Success
10000	1	Controller	0.1s	42.44	42.44	-0.11	-0.11	Fail
10000	1	Controller	1s	41.09	41.09	-1.46	-1.46	Success
10000	1	Controller	2s	40.08	40.74	-2.47	-1.81	Success
10000	1	Controller	3s	40.01	40.57	-2.54	-1.98	Success
10000	1	Actuator	0.1s	42.43	42.43	-0.12	-0.12	Fail
10000	1	Actuator	1s	41.14	41.14	-1.41	-1.41	Success
10000	1	Actuator	2s	40.84	40.84	-1.71	-1.71	Success
10000	1	Actuator	3s	40.71	40.71	-1.84	-1.84	Success

Table B.13: v_{x0} = 43km/h, F_{brake}^{req} = -20000N, VTM t_0 = 43.4s, sample time = 0.01s

Total request brake force (N)	τ_{pred}	Desired Force	Predict Horizon	Predict t_1 (s)	Predict t_2 (s)	Δt_1 (s)	Δt_2 (s)	Action prevent jack-knife
20000	0.2	Request	0.1s	43.26	43.26	-0.14	-0.14	Fail
20000	0.2	Request	1s	40.01	40.01	-3.39	-3.39	Success
20000	0.2	Request	2s	40.01	40.01	-3.39	-3.39	Success
20000	0.2	Request	3s	40.01	40.01	-3.39	-3.39	Success
20000	0.2	Controller	0.1s	43.33	43.33	-0.07	-0.07	Fail
20000	0.2	Controller	1s	40.01	40.83	-3.39	-2.57	Success

20000	0.2	Controller	2s	40.01	40.46	-3.39	-2.94	Success
20000	0.2	Controller	3s	40.01	40.3	-3.39	-3.1	Success
20000	0.2	Actuator	0.1s	43.33	43.33	-0.07	-0.07	Fail
20000	0.2	Actuator	1s	40.95	40.95	-2.45	-2.45	Success
20000	0.2	Actuator	2s	40.63	40.63	-2.77	-2.77	Success
20000	0.2	Actuator	3s	40.49	40.49	-2.91	-2.91	Success
20000	1	Request	0.1s	43.31	43.31	-0.09	-0.09	Fail
20000	1	Request	1s	40.07	40.07	-3.33	-3.33	Success
20000	1	Request	2s	40.01	40.01	-3.39	-3.39	Success
20000	1	Request	3s	40.01	40.01	-3.39	-3.39	Success
20000	1	Controller	0.1s	43.34	43.34	-0.06	-0.06	Fail
20000	1	Controller	1s	40.91	40.91	-2.49	-2.49	Success
20000	1	Controller	2s	40.01	40.52	-3.39	-2.88	Success
20000	1	Controller	3s	40.01	40.35	-3.39	-3.05	Success
20000	1	Actuator	0.1s	43.33	43.33	-0.07	-0.07	Fail
20000	1	Actuator	1s	40.95	40.95	-2.45	-2.45	Success
20000	1	Actuator	2s	40.63	40.63	-2.77	-2.77	Success
20000	1	Actuator	3s	40.49	40.49	-2.91	-2.91	Success

Table B.14: v_{x0} = 43km/h, F_{brake}^{req} = -30000N, VTM t_0 = 43.36s, sample time = 0.01s

Total request brake force (N)	τ_{pred}	Desired Force	Predict Horizon	Predict t_1 (s)	Predict t_2 (s)	Δt_1 (s)	Δt_2 (s)	Action prevent jack-knife
30000	0.2	Request	0.1s	43.2	43.2	-0.16	-0.16	Success
30000	0.2	Request	1s	40.01	40.01	-3.35	-3.35	Success
30000	0.2	Request	2s	40.01	40.01	-3.35	-3.35	Success
30000	0.2	Request	3s	40.01	40.01	-3.35	-3.35	Success
30000	0.2	Controller	0.1s	40.01	43.29	-3.35	-0.07	Success
30000	0.2	Controller	1s	40.01	40.78	-3.35	-2.58	Success
30000	0.2	Controller	2s	40.01	40.4	-3.35	-2.96	Success
30000	0.2	Controller	3s	40.01	40.24	-3.35	-3.12	Success
30000	0.2	Actuator	0.1s	43.28	43.28	-0.08	-0.08	Success
30000	0.2	Actuator	1s	40.9	40.9	-2.46	-2.46	Success
30000	0.2	Actuator	2s	40.57	40.57	-2.79	-2.79	Success
30000	0.2	Actuator	3s	40.42	40.42	-2.94	-2.94	Success
30000	1	Request	0.1s	43.25	43.25	-0.11	-0.11	Success
30000	1	Request	1s	40.01	40.01	-3.35	-3.35	Success
30000	1	Request	2s	40.01	40.01	-3.35	-3.35	Success
30000	1	Request	3s	40.01	40.01	-3.35	-3.35	Success
30000	1	Controller	0.1s	43.28	43.28	-0.08	-0.08	Success

30000	1	Controller	1s	40.01	40.29	-3.35	-3.07	Success
30000	1	Controller	2s	40.01	40.46	-3.35	-2.9	Success
30000	1	Controller	3s	40.01	40.85	-3.35	-2.51	Success
30000	1	Actuator	0.1s	43.28	43.28	-0.08	-0.08	Success
30000	1	Actuator	1s	40.9	40.9	-2.46	-2.46	Success
30000	1	Actuator	2s	40.56	40.56	-2.8	-2.8	Success
30000	1	Actuator	3s	40.42	40.42	-2.94	-2.94	Success

DEPARTMENT OF SOME SUBJECT OR TECHNOLOGY
CHALMERS UNIVERSITY OF TECHNOLOGY
Gothenburg, Sweden
www.chalmers.se

CHALMERS
UNIVERSITY OF TECHNOLOGY